Photonik
Ingenieurbüro
Dr. Walter Luhs

UM-LE-03 Manual for

HeNe-Laser-V2022

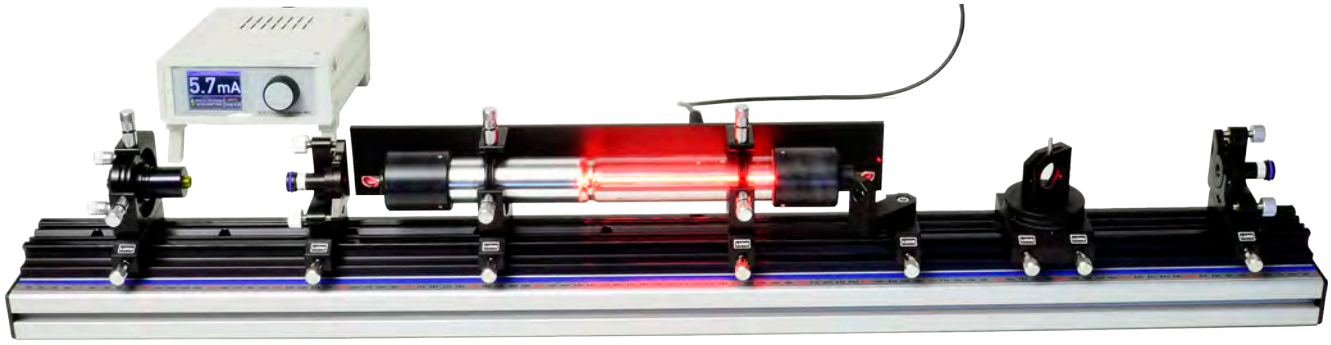

Table of Contents

1.0 Introduction

The first ever operated laser was an optically pumped solid state laser. This laser has been discovered by Theodore Maiman in 1960 [1]. The active material was the element #24, the Chromium, which was embedded into a transparent host crystal. The host crystal is a transparent corundum crystal also known as Aluminium oxide (Al_2O_3). The Chromium dopant replaces some Aluminium atoms thus changing the optical properties of the crystal. The so doped crystal shows a red colour and is also known as ruby.

^{1}H																	^{2}He
^{3}Li	^{4}Be											^{5}B	^{6}C	^{7}N	^{8}O	^{9}F	^{10}Ne
^{11}Na	^{12}Mg											^{13}Al	^{14}Si	^{15}P	^{16}S	^{17}Cl	^{18}Ar
^{19}K	^{20}Ca	^{21}Sc	^{22}Ti	^{23}V	^{24}Cr	^{25}Mn	^{26}Fe	^{27}Co	^{28} Ni	^{29}Cu	^{30}Zn	^{31}Ga	^{32}Ge	^{33}As	^{34}Se	^{35}Br	^{36}Kr
^{37}Rb	^{38}Sr	^{39}Y	^{40}Zr	^{41}Nb	^{42}Mo	^{43}Tc	^{44}Ru	^{45}Rh	^{46}Pd	^{47}Ag	^{48}Cd	^{49}In	^{50}Sn	^{51}Sb	^{52}Te	^{53}I	^{54}Xe
^{55}Cs	^{56}Ba	57..71	^{72}Hf	^{73}Ta	^{74}W	^{75}Re	^{76}Os	^{77}Ir	^{78}Pt	^{79}Au	^{80}Hg	^{81}Tl	^{82}Pb	^{83}Bi	^{84}Po	^{85}At	^{86}Rn
^{87}Fr	^{88}Ra	89..103	^{104}Rf	^{105}Db	^{106}Sg	^{107}Bh	^{108}Hs	^{109}Mt	^{110}Ds	^{111}Rg	^{112}Cn	^{113}Uut	^{114}Fl	^{115}Uup	^{116}Lv	^{117}Uus	^{119}Uuo
		↓															
		^{57}La	^{58}Ce	^{59}Pr	^{60}Nd	^{61}Pm	^{62}Sm	^{63}Eu	^{64}Gd	^{65}Tb	^{66}Dy	^{67}Ho	^{68}Er	^{69}Tm	^{70}Yb	^{71}Lu	
		^{89}Ac	^{90}Th	^{91}Pa	^{92}U	^{93}Np	^{94}Pu	^{95}Am	^{96}Cm	^{97}Bk	^{98}Cf	^{99}Es	^{100}Fm	^{101}Md	^{102}No	^{103}Lr	

Table 1: Periodic table of the elements

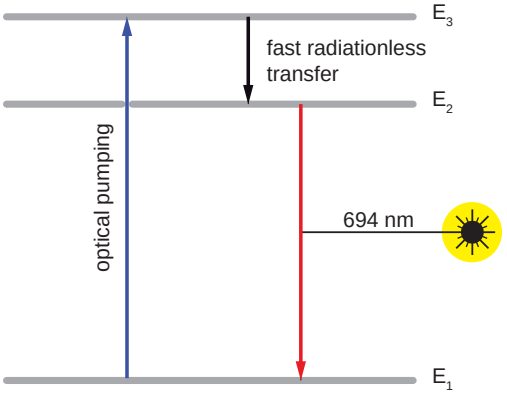

Fig. 1: Simplified three level system of the ruby laser

The ruby laser boosted a tremendous research and initiated a hunt for other more promising laser materials. One of the major drawbacks of the ruby laser was the fact that it could only operate in pulsed mode. This is due to its three laser level system as shown in Fig. 1.1. By excitation with suitable light Chromium ions of the ground state (E_1) are excited and consequently populate the excited state (E_3). From here the only way back to the ground state is via the E_2 energy level. In a first step the excited Cr ions are transferring a fraction of their energy to the lattice of the host crystal and are assembling in the energy level E_2. The transfer from $E_3 \rightarrow E_2$ is very fast and takes place in a few picoseconds. Population inversion is hard to achieve in a three energy level system like the ruby laser. However, the energy level E_2 is a so called metastable state. That means that the Cr ions are trapped in this state, since an optical transition to the ground state is forbidden due to the rules of quantum mechanics. Nature is not strictly merciless and a forbidden transition still has a certain probability and can be considered as a weak optical transition. Nevertheless the Cr ions will remain approximately 5 micro seconds in the E_2 state (which is fairly long for optical transitions) before they reach the ground state again.

$$(N_2 - N_1) = \frac{2\pi n^2 \nu^2}{c^2} \quad \textbf{(1)}$$

We learned that a laser process can only start, if the so called Schawlow-Townes oscillation condition [2] is fulfilled. The equation (1) shows a simplified version of it. In this equation n stands for the index of refraction, ν for the laser frequency and c for the speed of light, N_2 is the population density of energy level E_2 and N_1 accordingly. Only if N_2-N_1 is greater zero the equation yields useful results. In other words the population density of state E_2 must be greater than that of state E_1. This situation is also termed as population inversion.

Such an inversion can hardly be reached since N_1 is the population of the ground state, which is always populated. Only under “hard pumping” most Cr ions will be transferred to E_2. We have just 5 microseconds time to almost empty the ground state before the delayed transfer from E_2 starts to populate the ground state.

This is one of the reasons that a ruby laser in general emits pulsed laser radiation. On the search for a more suitable laser material the element #60 (Neodymium) turned out to be a good candidate. Laser operation of Neodymium was first demonstrated by J. E. Geusic et al. at Bell Laboratories in 1964 [5].

However, in the same year of the invention of the Ruby laser Ali Javan in December of 1960 [4] discovered the first gas laser operating in continuous wave mode (cw).

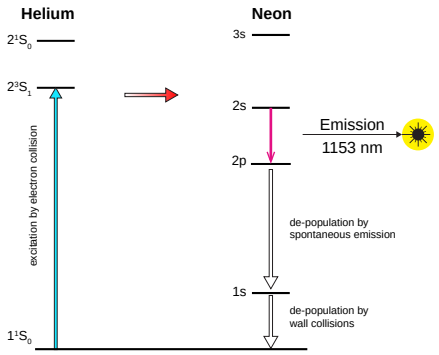

Fig. 2: Laser cycles firstly operated by Ali Javan [4]

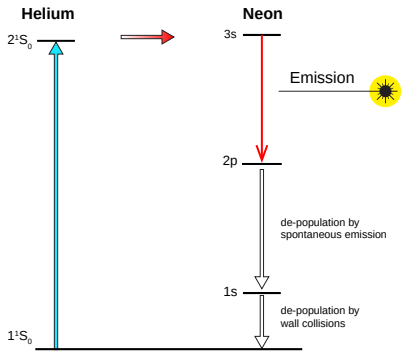

Fig. 3: Visible laser emission as operated by [6] in 1962 in an transparent manner

.

The outstanding property of such a HeNe laser lies in the fact that the laser process takes place inside a sort of a 4 level energy system [Fig. 2]. This and the extreme purity and coherence of the laser emission made this laser to an indispensable tool for a great variety of applications. Although the diode laser took over a great range of applications, the HeNe laser is still used in all air craft for GPS independent navigation and for highly precise laser metrological applications like industrial laser interferometer for the calibration of CNC machines.

Furthermore this laser system is an integral part of the lectures worldwide in photonics since it is based on atomic energy levels and teaches about the operation of a laser cavity

From the Fig. 2 we can conclude that the laser oscillation condition (1) is already fulfilled once the excitation takes place. In this system the population inversion is created between the energy levels 2s and 2p (Javan) or 3s and 2 p and since the 2p energy level is far above the ground state its population is zero. So even a single excited 2s or 3s Neon atom provides an population inversion.

2.0 Helium Neon Laser

2.1 Energy level system

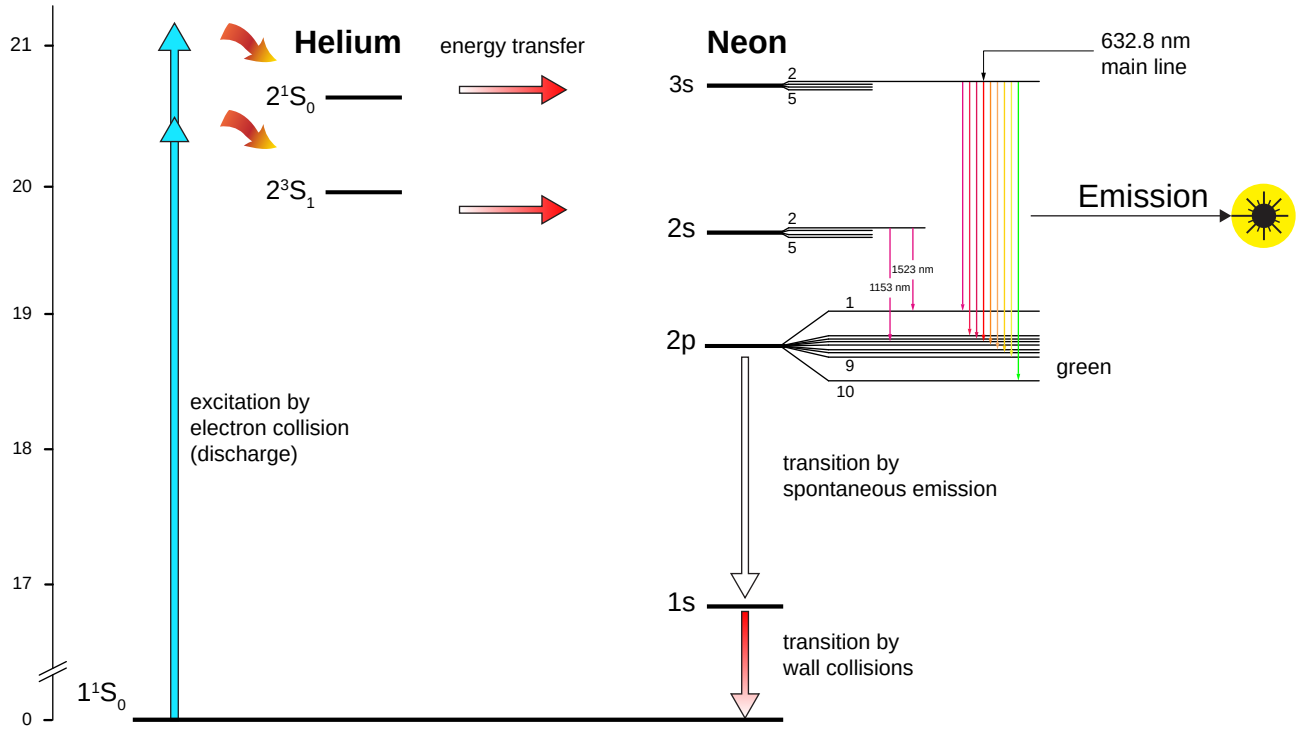

Fig. 4: Simplified energy level diagram of the He Ne laser system

When the quantum mechanics was been born and accepted, its validity has to be verified that it was able to describe the nature. It was no wonder that one started with simple atoms like Hydrogen (H), Helium (He) and Neon (Ne) since the mathematical complexity dramatically increased with atoms having multiple electron considering all possible interaction. As a result of this the spectroscopic data of He and Ne have been known very precisely. Based on this Javan et. al. tried the He Ne system at first. It was already known by this time that the 2^1S_0 and the 2^3S_0 states of the Helium are so called metastable. That means that from here no optically transitions are possible to the ground state. It means also that all transitions from higher lying states of the Helium will be trapped in thess two states. The excitation by the electrical discharge is a broad excitation which means that all possible states of the Helium are excited, however all transitions are terminating in these two metastable states 2^1S_0 and 2^3S_0.

And this is the trick of the Helium Neon laser which is not discussed commonly in text books. Many times, students raise the question, ***"…. why not excite the Neon directly by discharge? Why do we need the Helium?"***

Assuming we are only using Neon atoms and exciting it by a gas discharge we would populate almost all states of it. Thus we are not able to create a population inversion which is

commonly required for the laser operation or in other words we cannot fulfil the Schawlow-Townes oscillation condition [2]. If into the discharge tube of the Neon we add Helium, even 10 times more than Neon we selectively populate the 3s and 2s states of the Neon via the 2^1S_0 and 2^3S_0 states of the Helium since this is the most efficient way of the Helium atoms to reach back to the ground state.
The combination of the trick of using Helium to obtain a population inversion in Neon and applying the spectroscopic data makes the invention of A. Javan even more admirable. A fascinating source to learn how this invention happened can be found by following the link mentioned at [3] of the bibliography on page 22.

2.2 Principle of operation

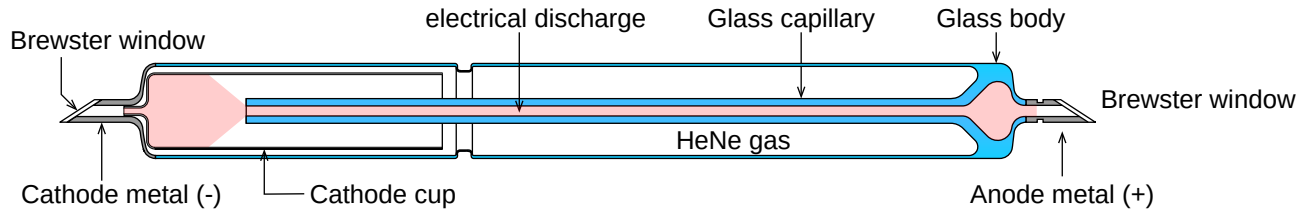

Fig. 5: Cut through a HeNe laser tube with Brewster widows on both sides

Each laser cycle can be described as a virtual flow of excited "particles". One nice method to do it is termed as rate equation model [7]. The idea is to identify and remove as far as possible "bottle necks" in the process. Even without applying the mathematics it can be recognised that the last step of the laser cycle of the Neon is the emptying of the 1s state to the ground state. The only way to do it is to let the excited Neon atoms run against a wall. That is why the Helium Neon laser requires the glass capillary. The 1s bottle neck is also the reason why the Helium Neon laser is limited to 50 -100 mW output power and never could become a high power laser. The task of the engineers was to find an optimum of a small capillary diameter and best mode volume match of the surrounding optical cavity.

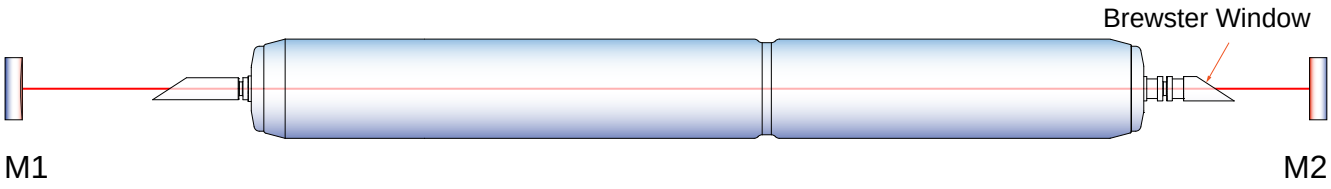

Fig. 6: Principle of open frame HeNe laser

An example of such a optimised laser tube is shown in [Fig. 6] and is the same one which is used in the experiments. Two Brewster windows are attached to the end of the tube. By adding two well aligned and coated mirrors an open frame HeNe resonator is formed. The complete experimental HeNe laser is described in the following chapter.

3.0 Experimental Set-up

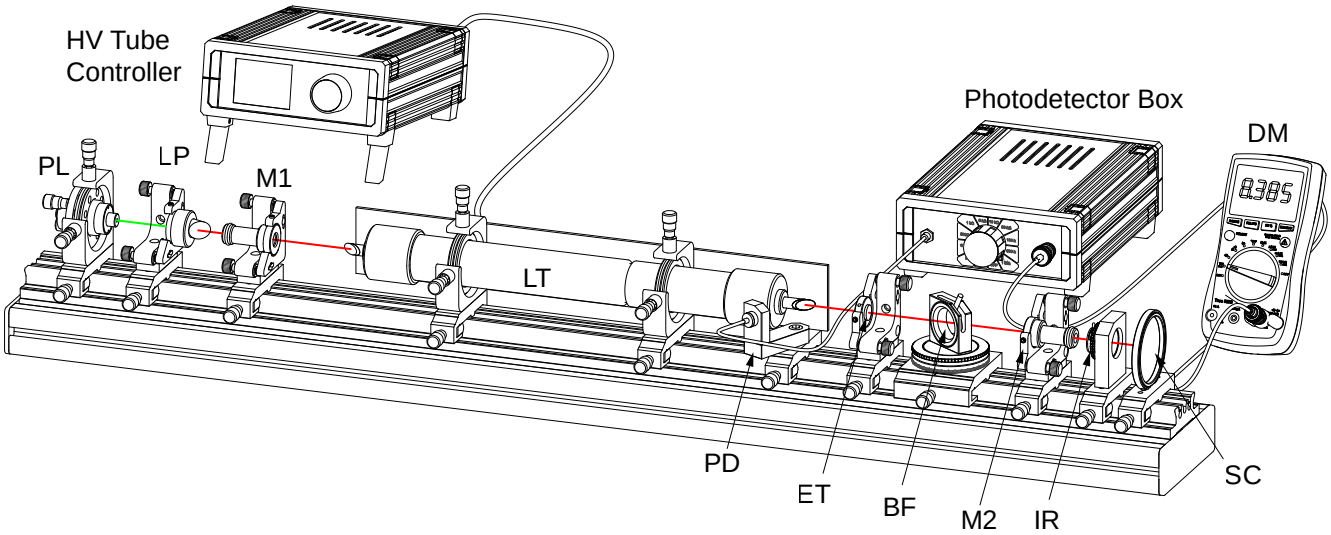

Fig. 7: Helium Neon Experimental Laser Setup

The figure above shows the setup using a precise optical rail and the modules for line selection as well as single mode operation. The individual components and modules are described in detail in the following chapters.

4.0 Description of the components

4.1 Optical rail

The rail and carrier system provides a high degree of integral structural stiffness and accuracy. Due to this structure it is a further development optimised for daily laboratory use. The optical height of the optical axis is chosen to be 65 mm above the table surface. The optical height of 32.5 mm above the carrier surface is compatible with all other systems like from MEOS, LUHS, MICOS, OWIS and LD Didactic. Consequently a high degree of system compatibility is achieved.

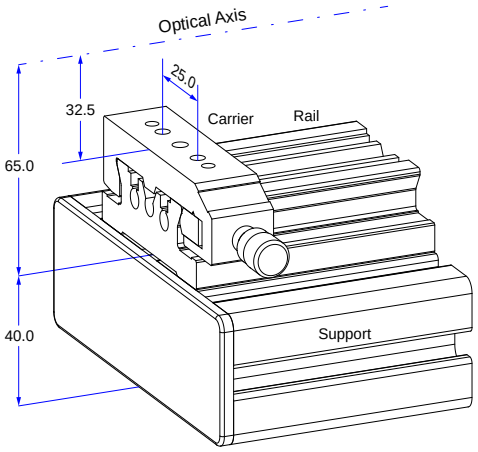

Fig. 8: Rail and carrier system

4.2 Pre-adjustment Laser PL

When Javan operated the first continuously operating laser he had no other laser to align the mirror of the cavity. At that time, a specialist accomplished this task experienced with interferometer and auto collimation telescopes. Nowadays, we use a green laser pointer which is mounted into a precise 4 axes adjustment holder.
By using four adjustment screws, the laser beam can be aligned orthogonally in XY direction and tilted in two orthogonal angles.

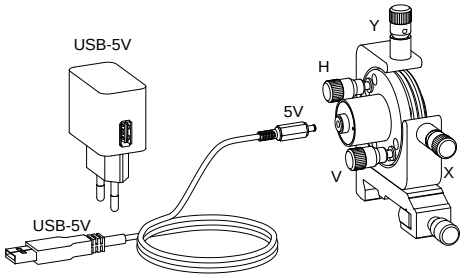

4.3 Laser mirror adjustment holder M1

The adjustment holder (AH) comprises two high precision fine pitch screws. The upper screw is used to tilt the moveable plate vertically and the lower one to tilt it horizontally.
The mounting plate provides a M16 mount into which the laser mirrors (LM) are screwed. The mirror is pressed against a mechanical reference plane inside the M16 mount in such a way that the mirror is always aligned perfectly when removed and screwed in again.
The adjustment holder is mounted to the carrier such that a “left” operating mode is achieved and thus forms the left mirror holder of the laser cavity.
Due to the symmetry of the adjustment holder (AH) it can also be changed to the “right” mode if required.

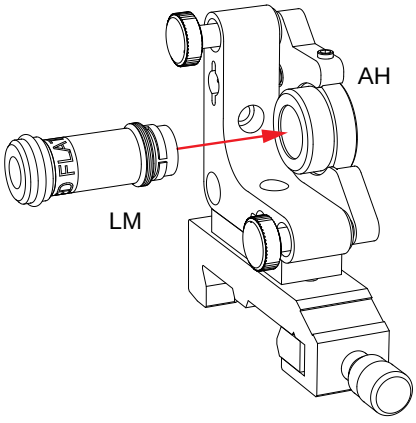

Fig. 9: Mirror adjustment holder “left”

4.4 Laser mirror adjustment holder M2

The adjustment holder (AH) comprises two high precision fine pitch screws. The upper screws is used to tilt the moveable plate vertically and the lower one to tilt it horizontally.
The mounting plate provides a M16 mount into which the laser mirrors (LM) are screwed. The mirror is pressed against a mechanical reference plane inside the M16 mount in such a way that the mirror is always aligned perfectly when removed and screwed in again.
The adjustment holder is mounted to the carrier such that a “right” operating mode is achieved and thus forms the right mirror holder of the laser cavity.
Due to the symmetry of the adjustment holder (AH) it can also be changed to the “left” mode if required.

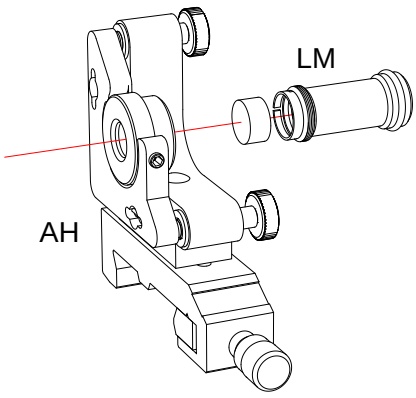

Fig. 10: Mirror adjustment holder “right”

4.5 Set of laser mirror

The set-up comprises two sets of mirrors each mounted separately as shown in Fig. 3.10. Each mirror has the standard diameter of 12.7 mm (½ inch) and a thickness of 6.35 mm (¼ inch).
The laser mirror (LM) is mounted into the holder MH and kept in position by two spring loaded flaps. A O-ring provides a soft seat of the mirror inside the holder (MH) especially when screwed into the adjustment holder.

The mirrors are of supreme quality, coated by ion beam sputtering (IBS) yielding the highest degree of reflectivity and lowest scatter losses achievable till date.
A cap (PC) protects the sensitive mirrors when not in use. Each mirror is labelled and the meaning of the marks is given in the right column.

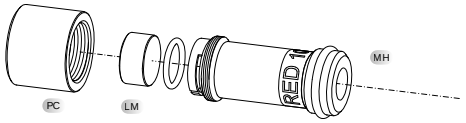

Fig. 11: Mounted laser mirror

Mark	Coating
RED	HR 580..720 nm
NIR	HR 1050 .. 1250 nm
HR	R > 99.98%
ROC	Radius of Curvature
Label	Geometry
RED FLAT	flat mirror
RED 750	ROC 750 mm
RED 1000	ROC 1000 mm
NIR FLAT	flat mirror
NIR 750	ROC 100 mm

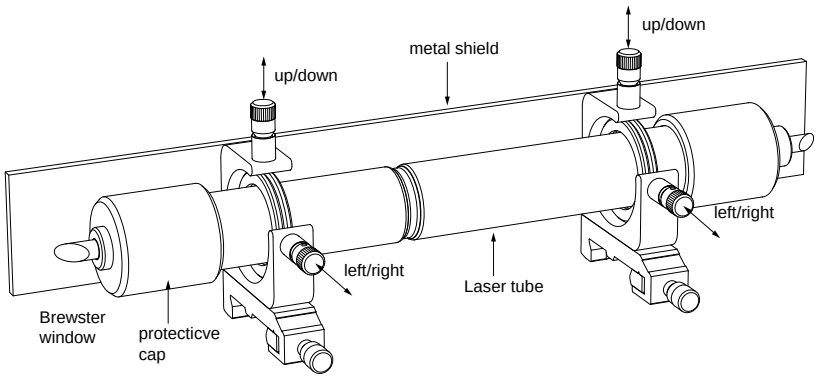

The laser tube is mounted into two XY adjustment holders. The tube can be aligned parallel to the X and Y direction as well as slightly tumbled along its axis. This is necessary to align the capillary with respect to the optical axis of the laser cavity.
A metallic shield carries on its rear the required ballast resistor for a stable high voltage discharge. Both the anode and cathode are insulated, so that no electrical hazard is possible. The Brewster windows are protected by soft silicon caps when the tube is not in operation.

4.6 Si PIN photodetector module (PD)

A Si PIN photodiode (PD) is integrated into a small housing and accommodated inside a mounting plate (MP), which attached to the swivel arm to take in the light reflected from the Brewster window. The photodiode is connected to the ZB1 box and detects low light intensities or fast signals up to 1 GHz to detect the beat frequency of the laser modes. It is connected via a BNC cable to the ZB1 box.

Parameter	Symbol	Value	Unit
Rise and fall time of the photo current at: R_L=50Ω; V_R=5 V; λ=850 nm and I_p=800 µA	t_r, t_f	20	ns
Forward voltage I_F = 100 mA, E = 0	VF	1.3	V
Capacitance at V_R = 0, f = 1 MHz	C0	72	pF
Wavelength of max. sensitivity	λ_{Smax}	850	nm
Spectral sensitivity S 10% of S_{max}	λ	1100	nm
Dimensions of radiant sensitive area	L × W	7	mm^2
Dark current, V_R = 10 V	IR	≤ 30	nA
Spectral sensitivity, λ = 850 nm	S(λ)	0.62	A/W

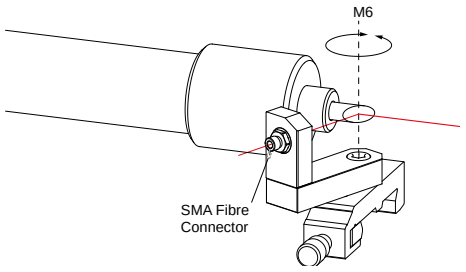

Fig. 12: Photodetector module PD

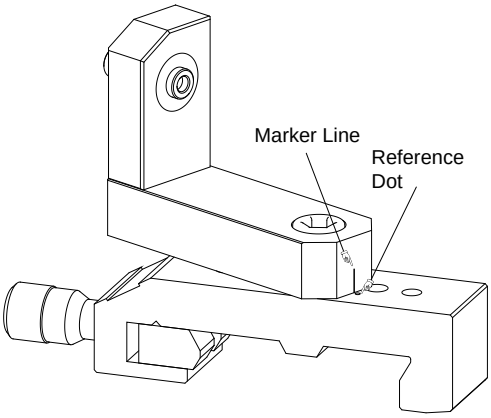

Fig. 13: Sensitivity curve $S_{rel}(\lambda)$

4.7 Photodetector Signal Box DC-0300

The signal box contains the photodiode, a resistor network and a replaceable 9V battery. The light is directed to the photodiode with an optical fibre. Based on the selected load resistor the sensitivity will be high for higher resistors but the rise and fall time will be longer. For fast signals a low resistor should be used, however the sensitivity will be lower.
More details please see chapter 7.0.

Fig. 14: Photodetector signal box

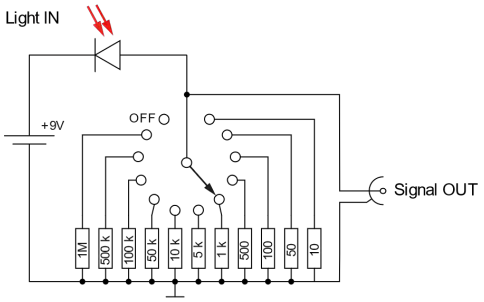

Fig. 15: Photodetector signal box schematic

4.8 Birefringent Tuner

A detailed description of the property and function of a double refractive tuning element can be found in [10] or [11].
The double refractive or birefringent plate (P) is mounted in a dual rotational stage. For the intra-cavity operation the birefringent plate (P) needs to be aligned in such a way that the laser beam hits the plate under the Brewster angle to minimize the reflection losses. This is accomplished by turning the rotary plate (B).
In addition the birefringent plate can be rotated around its optical axis by tilting the lever (L).
By rotating the plate (P) its optical retardation δ is changed. If the retardation of two passes is a multiple integer of the wavelength λ

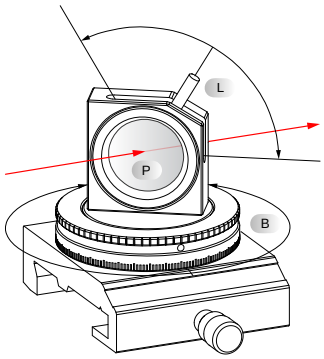

Fig. 16: Optional birefringent tuner

4.9 Littrow prism tuner

Another way to select different lines of a laser is to use a Littrow prism. A detailed description of tuning a HeNe Laser with a Littrow prism is given by Luhs [11].
Within this experiment we are using such a module to tune the Helium Neon laser. The Littrow is made from fused silica which is the required substrate for IBS coating.
The spectral range of the IBS coating covers 580..720 nm with a reflectivity >99.98 %. The prism is mounted into a precise adjustment holder where it can be smoothly tilted in vertical or horizontal direction.

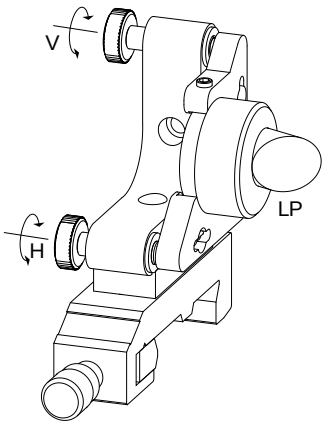

Fig. 17: Optional Littrow prism tuner

4.10 Single Mode Etalon

To force the laser to operate in only one longitudinal mode a so called etalon is used. It consists of a quartz cylinder which end faces are precisely ground parallel within a few arc seconds. The length is designed so that the convolution of its free spectral range with the HeNe cavity favours only one mode.
The etalon is mounted into a holder which is inserted into the adjustment holder. The provided hexagon key is used to fix the etalon mount. Two precise fine pitch screws allow the sensitive tilt of the etalon which is required to tune it inside the cavity to different orders of the etalon.
Further details or the properties of such an etalon can be found in [11] and in the chapter 5.9 of this manual.

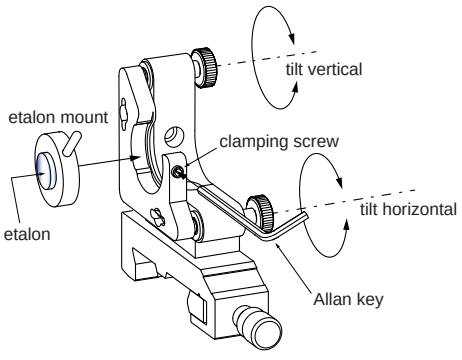

4.11 High voltage controller

A novel and safe combination of high voltage and micro processor control form the high voltage controller. The HeNe laser tube is connected via a special high voltage BNC connector to rear of the controller. The precision 5 turn potentiometer sets the discharge current in a range from 4.5 to 7 mA. When the external 12 V are applied the controller starts while displaying the screen as shown in Fig. 3.23. This will take approximately 3.5 seconds. After that the user is requested to authorize himself by entering the 4 digit pin code.

Fig. 18: Start-up screen

4.11.1 Laser Safety

The first interactive screen requires the log-in to the device, since due to laser safety regulations unauthorized operation must be prevented. In general this is accomplished by using a mechanical key switch. However, this microprocessor operated device provides a better protection by requesting the entry of a PIN.

After entering the proper key, the next screen is displayed and the system is ready for operation. The key is a 4 digit number, which can be changed by the user. For this purpose, enter the correct key (the ENTER key is highlighted). Touch the “CLEAR” button to clear the displayed key. Enter the new key and once it is complete, the “SAVE” button is enabled and can be touched.

If the key has been changed without giving notice to the responsible lab manager, there exists a method to read the key from the system. However, this method is not published here, it is given separately to the device upon delivery.

Fig. 19: Entry screen

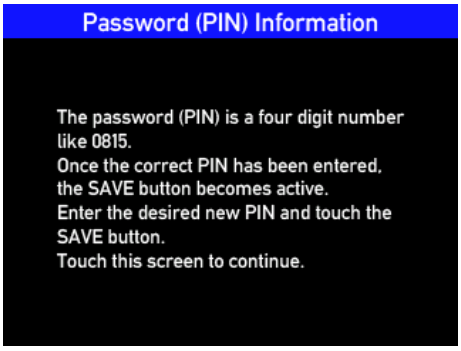

4.11.2 Main screen

When tapping the “Start the Discharge of the Laser Tube” a confirmation screen appears to confirm that the high voltage connector of the tube is firmly conected to the controller. After the confirmation the start process begins and after a time delay of 1.5 seconds the start voltage of 8 kV is applied to the tube. If the tube does not start within the next 0.5 seconds, the controller switches the high voltage as well as the 12 VDC for the high voltage module completely off.
Once successfully started the discharge tube can be set by turning the knob of the 5 turn potentiometer. The controller measures and displays the real tube current flowing across the tube.

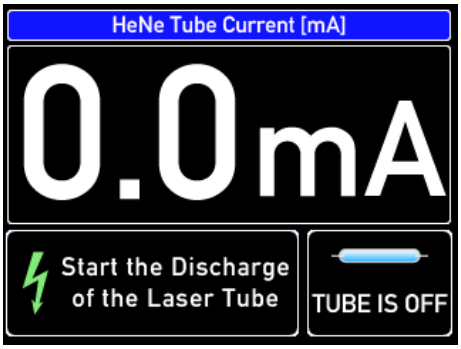

Fig. 20: Main screen

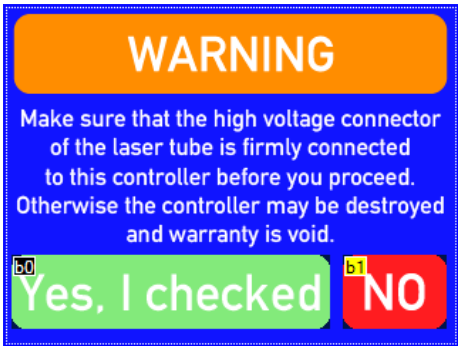

Fig. 21: Confirmation screen

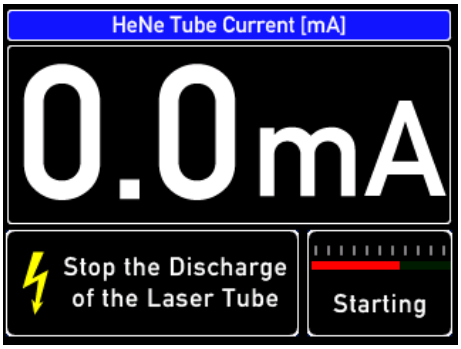

Fig. 22: Start the discharge

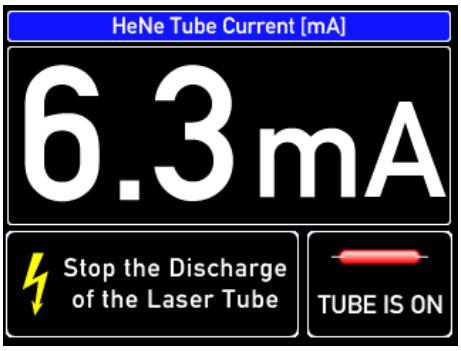

Fig. 23: Discharge is ON

4.11.3 Failure screen

If the tube does not start within 2 seconds than the failure screen shows up. It is advising to connect the tube to the controller if not done before.

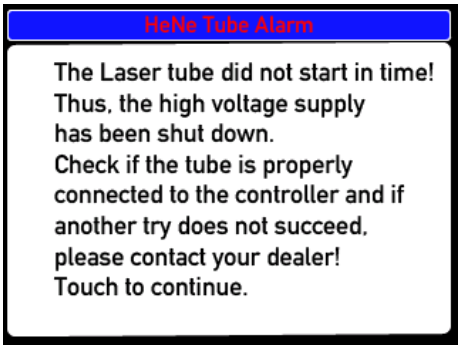

Fig. 24: Laser tube warning screen

5.0 Experimental set-up and Measurements

It is the aim to setup and align the HeNe laser and perform a variety of measurement tasks.

5.1 Basic alignment

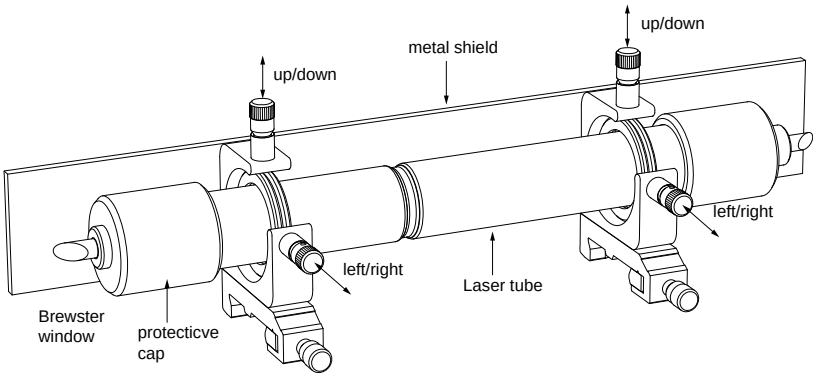

Fig. 25: HeNe Laser tube

The laser tube is visually centred to the mechanical axes of the adjustment holder, this forms the reference for all other components and defines the direction of the capillary.
Once the system is operating the adjustment screws can be used to optimise the laser cavity

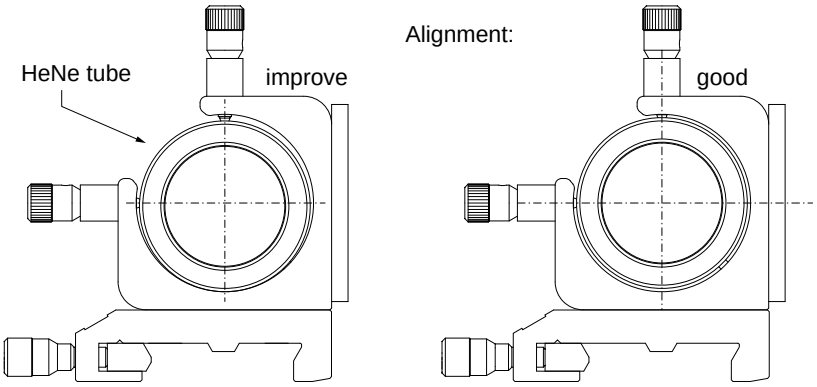

Fig. 26: Centric tube alignment

Centre the tube

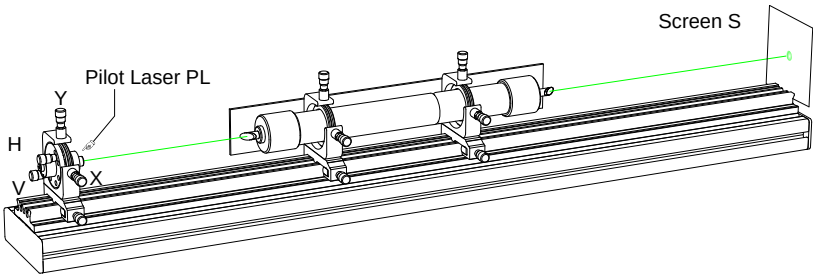

Fig. 27: Align the pilot laser

Pilot Laser alignment

Place the prepared laser tube onto the rail. Align the pilot laser in such a way that the green laser passes through the capillary of the HeNe tube unhindered.
Check this with a sheet of white paper or the image on the wall of the lab.

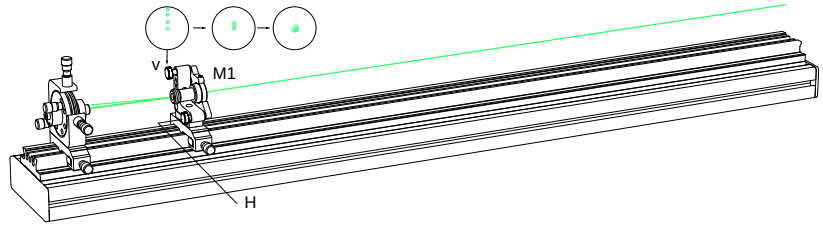

Fig. 28: Alignment of left mirror M1

Align the left mirror

Now the green laser beam is the reference for the capillary as well as for the rest of the components.
Insert the flat mirror and align its back reflex so that they coincide all as shown in the figure on the left.

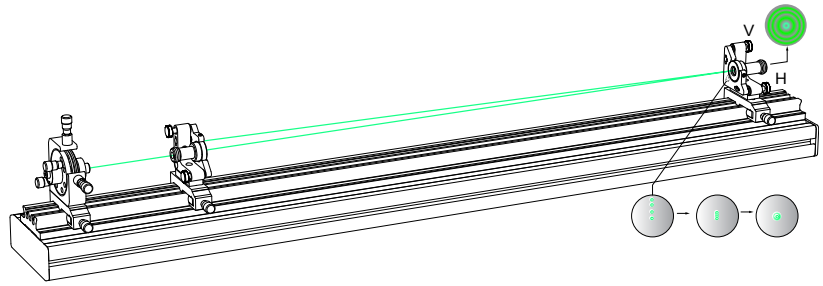

Fig. 29: Alignment of right mirror M2

Align the right mirror

It is good practise to start with the mirror having a radius of curvatures of 750 mm. Also centre the reflected beam to the green spot of the flat mirror.
Image the green beams again on a piece of white paper or watch it on the lab's wall. When properly aligned the cavity becomes resonant for the green and shows the Fabry Perot rings.

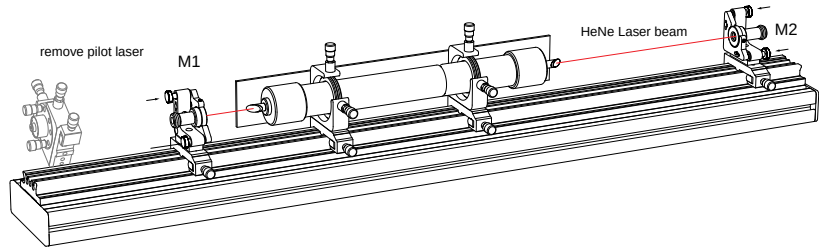

Fig. 30: Placing the HeNe tube

Start the laser

Place the tube between both mirrors in such a way that the left side of the tube is close to the flat mirror. In the section of Gaussian beams, we will learn why this is the best choice.
Switch on the discharge and the laser starts. Visually realign all adjustment screws for highest laser power.

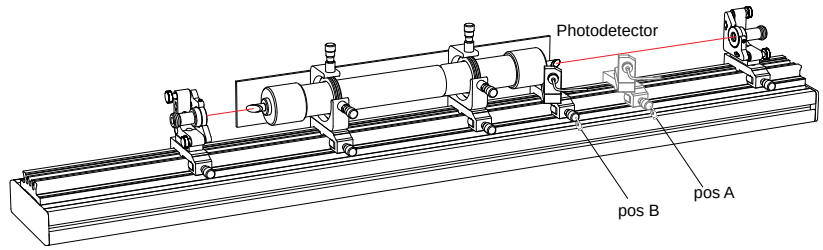

Fig. 31: Adding the photodetector module

Add the photodetector

Now the photodetector is added. Make sure that the beam hits the sensitive area of the detector. Maybe the tube must be slightly turned in its holder to direct the reflex from the Brewster window to the centre of the detector.

5.2 Optical stability criteria

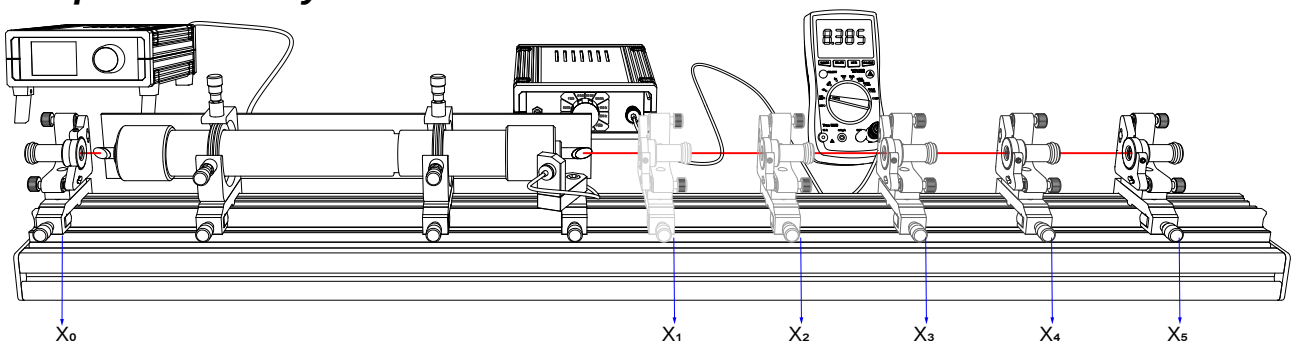

Fig. 32: Determination of the optical stability of the cavity

The stability criterion for optical cavities was introduced by Kogelnik and Li [8] is derived as

$$0 \le g_l \cdot g_2 \le 1$$

whereby

$$g_i = 1 - \frac{L}{R_i}.$$

L is the distance between the mirror and R_i is the radius of curvature of mirror M_i. In our setup we are using a flat mirror on the left side and a curved one on the right side. In the first setup we will use the mirror having a radius of curvature R of 750 mm. The stability criterion of resulting hemispherical cavity therefore is

$$0 \le \left(1 - \frac{L}{R_{left}}\right) \cdot \left(1 - \frac{L}{R_{right}}\right) \le 1$$

$$0 \le \left(1 - \frac{L}{0.75m}\right) \le 1$$

That means, that valid values of L, the distance between the mirrors, are within 0 .. 0.75 m. Calculating the same for 1 m of radius of curvature of the right mirror yields 1 m as maximum mirror distance.

To verify these findings we are taking for both mirrors the output power versus the mirror distance L as shown in [5.3]

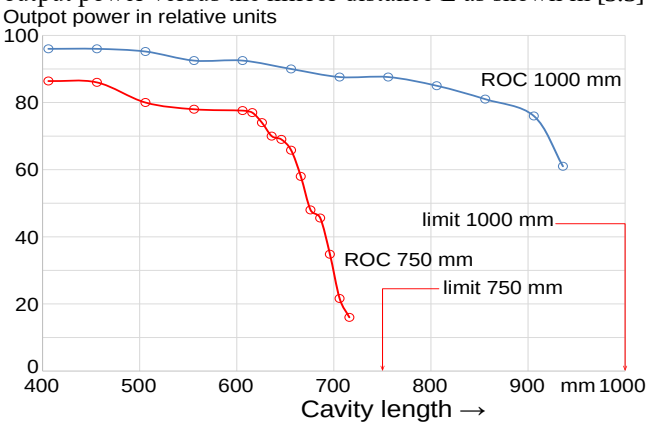

Fig. 33: Verification of the stability criterion or radius of curvature (ROC) 750 and 1000 mm

5.3 Gaussian beams

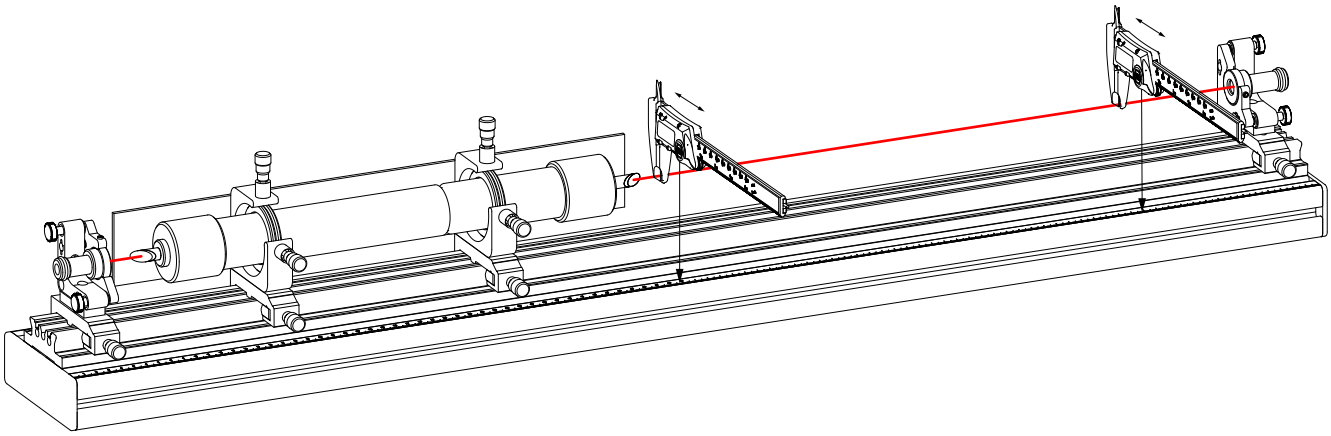

Fig. 34: Measuring the beam diameter inside the cavity

Useful equations:

$$w_1^2 = \frac{d \cdot L}{\pi} \cdot \sqrt{\frac{g_2}{g_1 \cdot (1 - g_1 \cdot g_2)}}$$

spot size at mirror M1. In our setup is g_1=1 and g_2 is 1-L/R. Since R = 1m g_2 is 1-L resulting in:

$$w_1^2 = \frac{L \cdot \lambda}{\pi} \cdot \sqrt{\frac{1 - L}{L}}$$

$$w_2^2 = \frac{L \cdot \lambda}{\pi} \cdot \sqrt{\frac{g_1}{g_2 \cdot (1 - g_1 \cdot g_2)}}$$

spot size at mirror M2

$$w_2^2 = \frac{L \cdot \lambda}{\pi} \cdot \sqrt{\frac{1}{(1 - L) \cdot L}}$$

$$w(z) = w_0 \cdot \sqrt{1 + \left(\frac{z}{z_R}\right)^2} \qquad z_R = \pi \cdot \frac{w_0^2}{\lambda}$$

This equation yields the beam waist as function of the position in side the cavity.

$$\theta = \frac{2 \cdot \lambda}{\pi \cdot w_0}$$

Far field angle

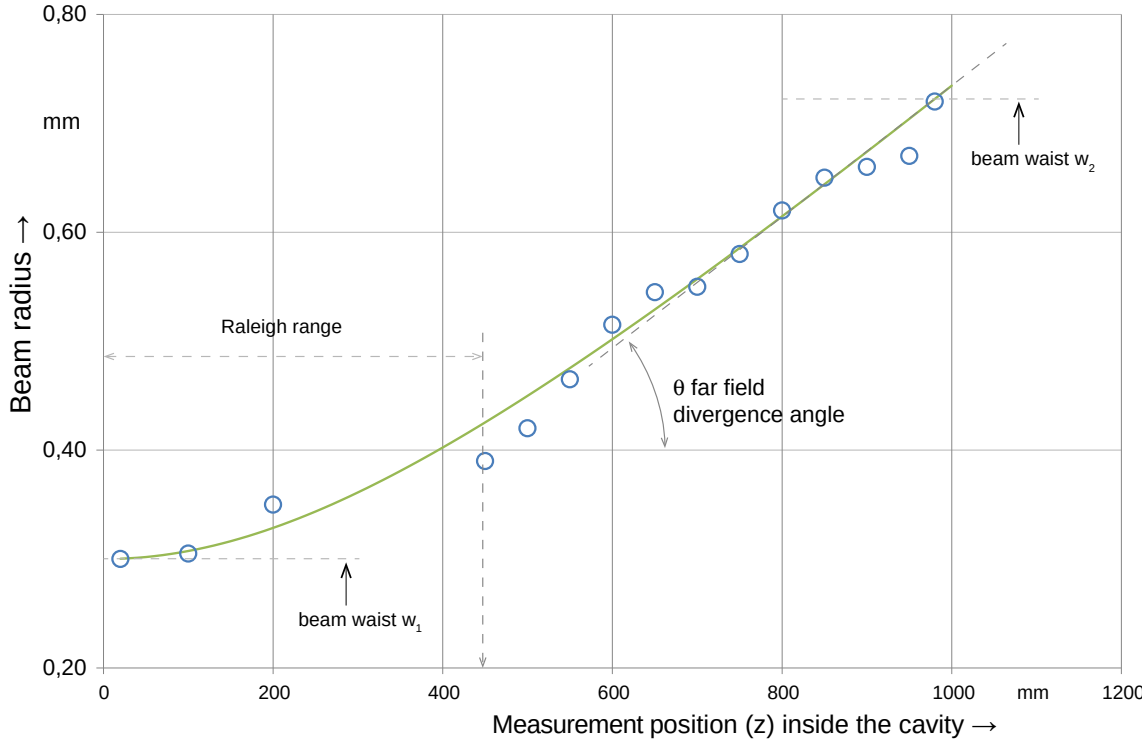

Fig. 35: Measured beam diameter as function of the position inside the cavity relative to left mirror

Within this experiment we verify that laser beam are Gaussian beams. The results can be compared to the calculated values using the set of equations given under “Useful equations”.

5.4 Excitation spectrum

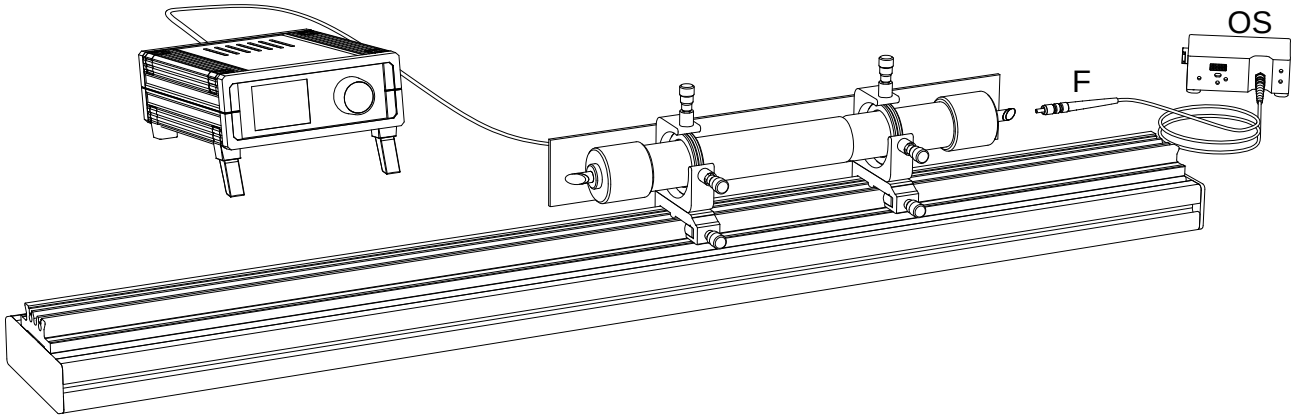

Fig. 36: Set-up to measure and record the excitation spectrum

We are using a spectrum analyser (OS) equipped with an optical fibre (F). The excitation fluorescence is so strong that holding the fibre in direction of the Brewster window an almost noise free signal will be detected. Such a spectrum is shown in Fig. 37.

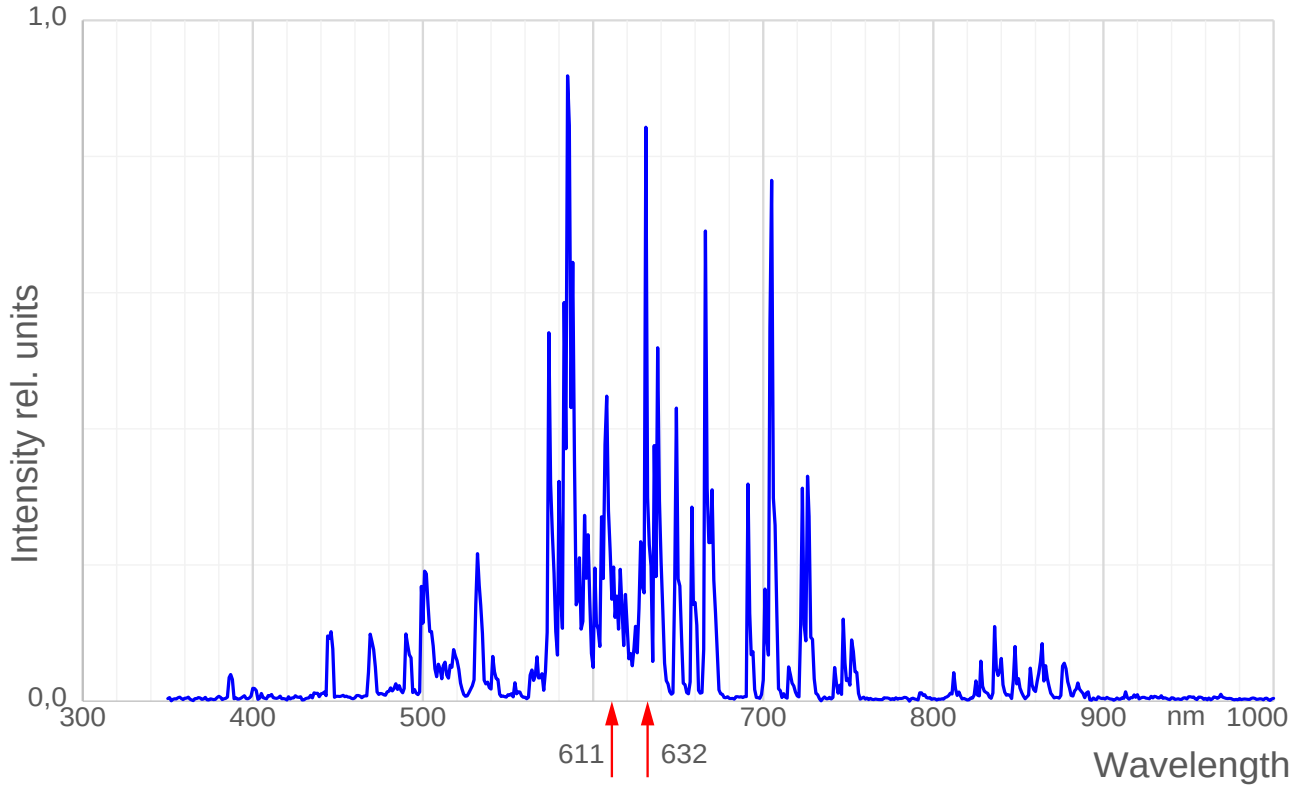

Fig. 37: Helium Neon fluorescence spectrum in the range of 350 ... 1000 nm

The resolution of the spectrum analyser is just 2 nm and a better one will yield more resolved lines. However, with this simple spectrum analyser the fluorescence lines can be assigned to the transitions of the energy level diagram as shown in Fig. 4.

5.5 Excitation of transverse modes*

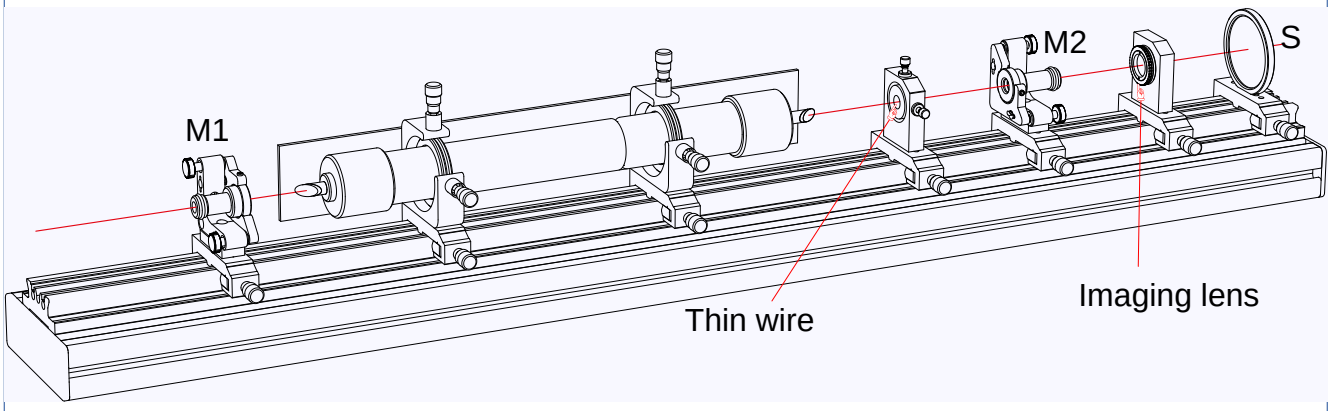

Fig. 38: Concentric cavity to support non-axial or transverse modes

Modern HeNe Laser tubes are optimised for high power output in TEM_{00} mode. The diameter of the internal capillary is an optimum of the diameter for laser power. Enlarging the diameter reduces the wall collision rate which is responsible for an efficient laser cycle (see Fig. 2 and Fig. 3). A small diameter seems to be better, but the mode volume is reduced, bringing down the power. This means, that the demonstration of transverse modes with such a commercial laser tube requires some extra means. First of all the mode volume must be increased, which is achieved by using a concentric cavity with the laser tube placed in the centre between both mirrors. Secondly a thin wire can be used to get a clearer separation of the nodes.

Fig. 39: Picture recorded from the rear of the translucent screen

To setup the concentric mode it is recommended to use two mirror (M1 and M2) with same radii of curvature. The experiment comes with mirror having 700 mm, that means the focus is at 350 mm. The concentric cavity requires that the two foci are at the same spot, or in other words, the mirror separation is 70 mm. In addition the translucent screen (S) is positioned at the rearmost end of the rail. The imaging lens consists of a biconcave lens with a focal length of -5 mm and strongly expands the laser beam for better visibility of the pattern of the transverse modes.

Once the laser is running (you will notice that the alignment of such a spherical cavity is easier than the hemispherical), always transverse modes will be observed even without the thin wire. The number of modes and pattern vary with the alignment of the mirror M1 and M2 as well as the position of the tube.

The pattern becomes clearer when the adjustable thin wire is placed inside the cavity. The wire is aligned in such a way, that the laser beam fully hits the wire. This creates a clear transverse mode structure on the screen. The structure can be changed by the mirror alignment, the distance of the mirrors and the position and orientation of the thin wire.

By using an ordinary digital camera as well as the standard camera of a mobile phone the image of the transverse modes can be taken from the rear of the translucent screen.

*The components which are required for the excitation of transverse modes are contained in the optional “OM-0596 Transverse Mode Enhancer”.

5.6 Wavelength selection and tuning

As already mentioned in chapter 2.0 the Helium Neon laser has the potential to oscillate on different wavelengths. The goal of this experiment is to tune to as much as possible of these wavelengths. In principle a laser oscillates on a wavelength for which the gain is the highest and losses are the lowest.

The gain is determined basically by the laser material the losses however, mainly by the laser cavity. Basically for each wavelength a set of mirrors with appropriate coating can be created, however this is a quite cumbersome way to select a specific wavelength. It would be much better just to turn a knob to tune to a different wavelength.

Such devices exist, one of it is the so called Littrow Prism and another one is the birefringent tuner. In the set-up of Fig. 42 we using a birefringent tuner which is simply placed into the cavity. To avoid any insertion losses the birefringent or double refractive plate is turned to the Brewster's angle.

5.7 Wavelength selection with Littrow prism

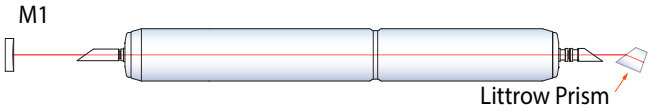

Fig. 40: Principle of Littrow prism tuning

Using a Littrow prism for laser line tuning requires a modification of the laser cavity since the reflecting surface of the prism is flat. Therefor the flat mirror will be exchanged against the Littrow prism. Otherwise it results in a cavity with two flat mirror. It is well known that such a cavity will be optically stable, however is extremely hard to align and to maintain laser oscillation.

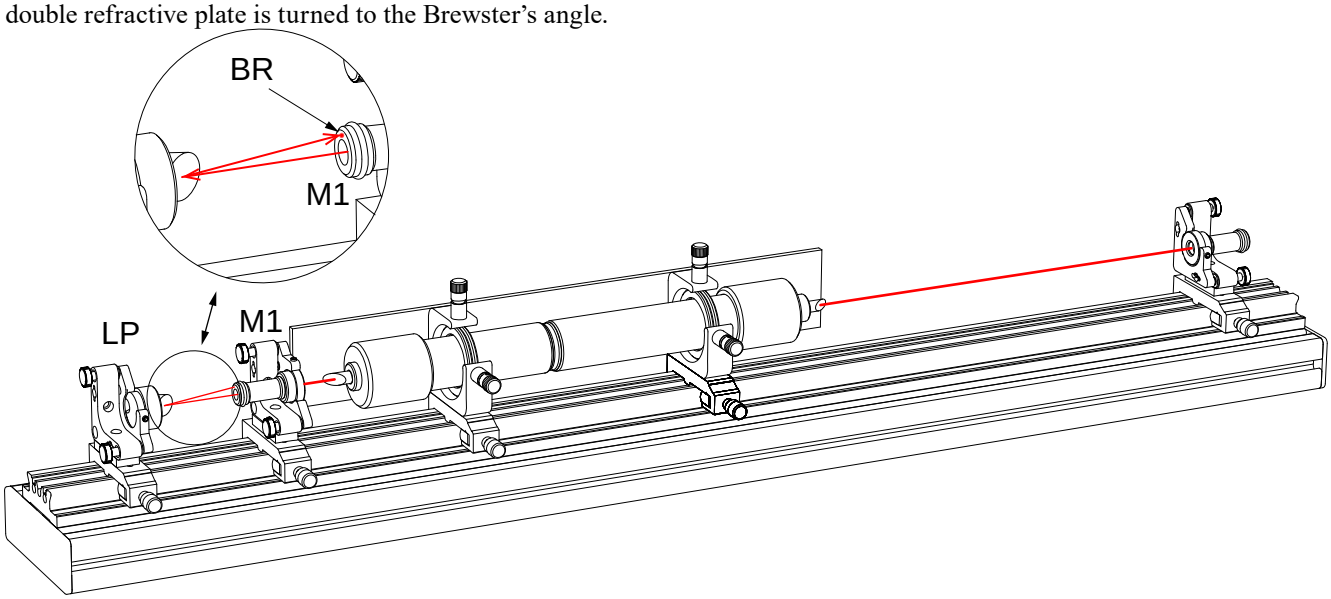

Fig. 41: Arrangement with Littrow prism tuner

It is good practise to align the Littrow prism (LP) with the laser beam which emerges from the left mirror M1. Simply align the reflex to the centre of the mirror mount. The closer that the alignment is reached, the more reflections appear. Optimum alignment is achieved when the back reflecting beam starts to flicker which indicates a close coupled cavity.

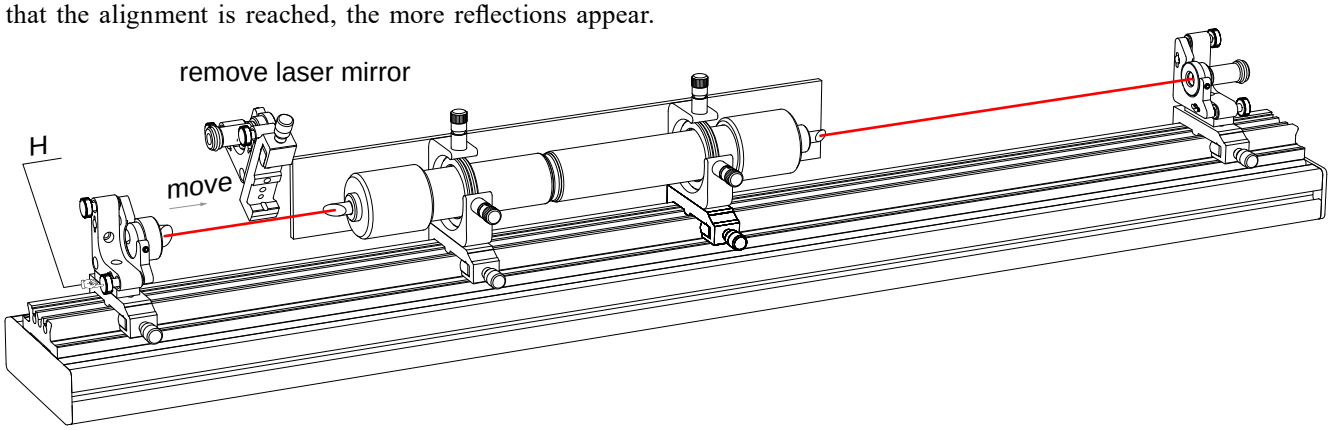

Remove the laser mirror M2. Now laser operation should occur with the Littrow prism. Align for maximum brightness. Move the Littrow prism as close as possible to the laser tube. Once the entire system is optimised one can start to tune to other lines by turning the fine pitch screw (H) for the horizontal tilting. **Also here it might be a good idea to clean the Brewster windows as well as the surface of the Littrow prism.**

5.8 Wavelength selection with BFT

Fig. 42: Principle of line tuning with a birefringent plate

The Brewster window forces the Helium Neon laser to operate on strictly polarised light. The inserted birefringent plate changes the polarisation due to its double refractive property. The losses at the Brewster window would create such high losses that the oscillation stops. If the birefringent plate is rotated around its axis the change of polarisation is different because the change of the polarisation depends on the phase retardation. However, if we set the plate to such an angle where the phase shift is just λ/2 the returning beam is shifted again by λ/2 resulting in a total phase shift of λ which means the polarisation is not influenced and the laser oscillates on that specific wavelength.

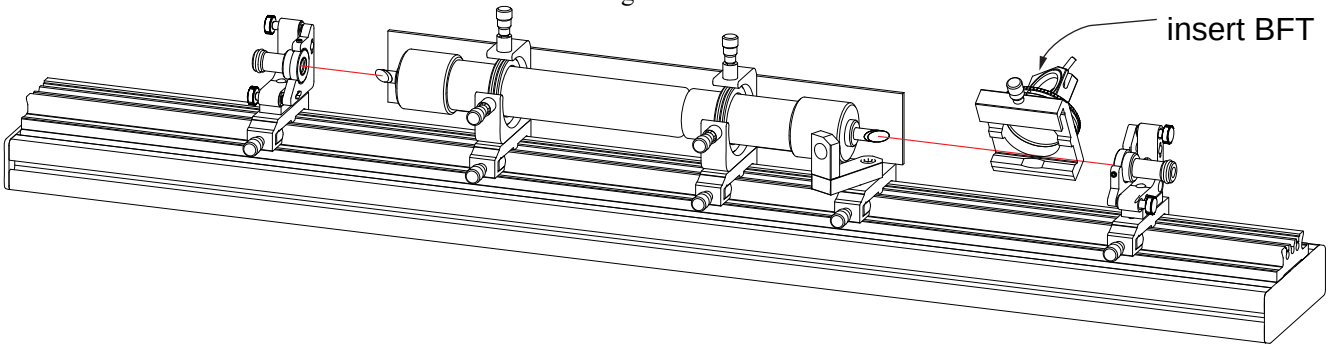

Fig. 43: In an optimised setup the birefringent tuner is inserted

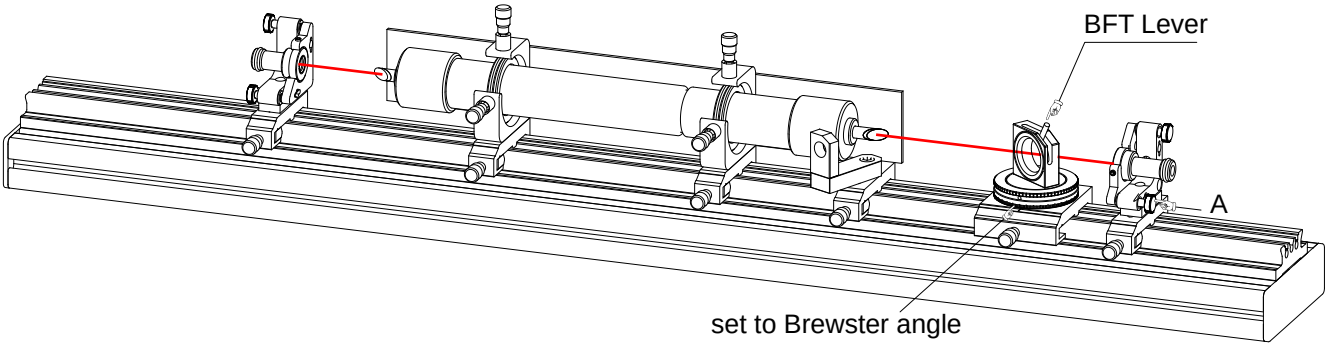

Fig. 44: Bringing back the laser oscillation

Set the birefringent plate to the Brewster angle (57°). When rotating the birefringent plate by tilting the lever (L) laser emission should occur. If not lift the lever up and down while adjusting the knob A to compensate the beam deviation caused by the quartz plate. Then gently tune to the maximum of performance and optimise the alignment of the mirror M2. By tilting the lever some other wavelength should show up. **It is very important that the Brewster window of the laser tube as well as the birefringent plate is cleaned and no dust particles are visible.**

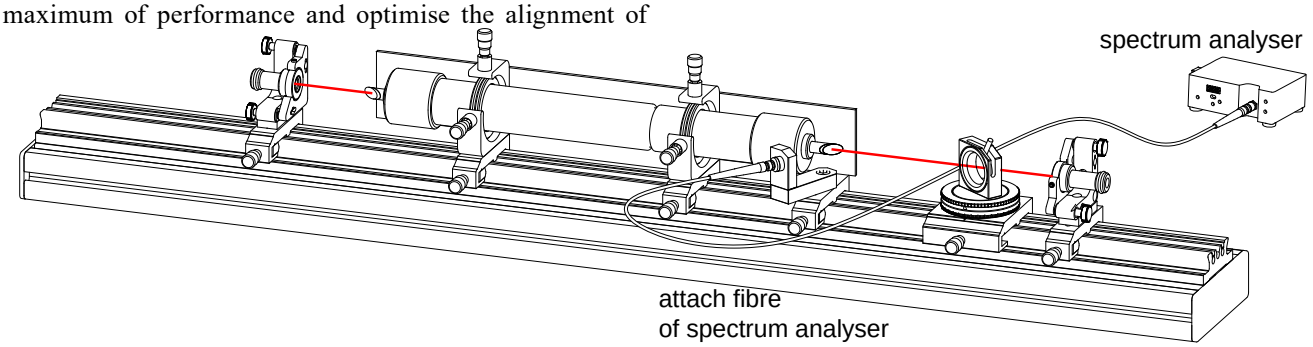

Fig. 45: Connect the fibre of the spectrum analyser by using the 12 mm SMA fibre adapter

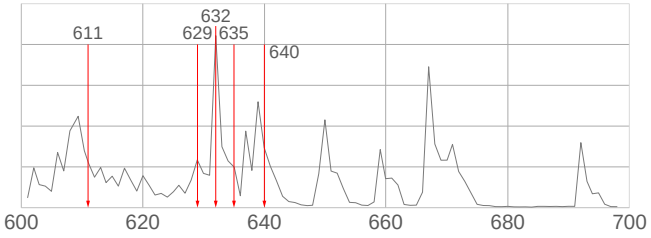

Fig. 46: Observed lines drawn into the fluorescence spectrum

By rotating the birefringent plate 5 lines can be observed. It is recommended to make use of such an optical spectrum analyser since the colour of the lines does not change significantly, except the orange line at 611 nm.

	Wavelength	*Strength*
A	611.8 nm	10
B	629.8 nm	20
C	632.8 nm	100
D	635.2 nm	6
E	640.1 nm	34

Table 2: Observable lines and relative strength

5.9 Single mode operation with etalon

A free running laser will operate on all possible cavity modes as long as gain is provided. Due to the inhomogeneous broadened gain profile [11] the Helium Neon laser can oscillate on a number of modes which are defined by the losses and the length L of the cavity.

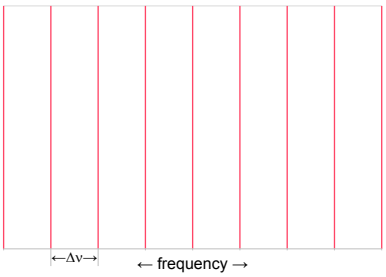

Fig. 47: Empty cavity

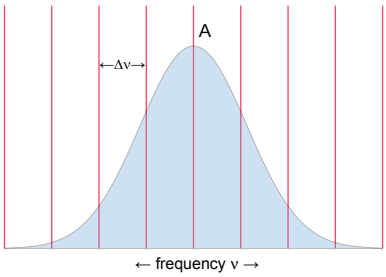

Fig. 48: Cavity with amplifying Neon

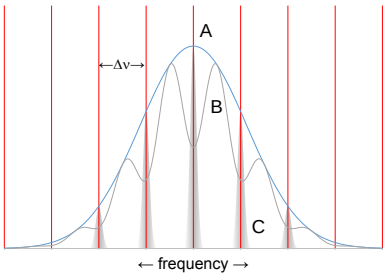

Fig. 49: Longitudinal multimode oscillation

An empty cavity with a mirror spacing of L can accommodate stable modes which fulfil the condition:

$$N \cdot \frac{\lambda}{2} = L$$

N is an integer and of course a large number considering the wavelength λ is 632 nm and the cavity length 1 m for example. There exist an infinitive number of such modes. The difference frequency $\Delta\nu$ of two neighboured modes is consequently:

$$\Delta\nu = \frac{c}{2 \cdot L}$$

If such a cavity is filled by amplifying Neon as shown in [Fig. 48], a couple of modes fit under the gain profile (A). Laser oscillation occurs when the losses are compensated by the gain resulting in so called hole burning of the gain profile (A) resulting in a modified gain profile (B). It becomes apparent, that for a number of modes, longitudinal modes, the oscillation condition can be fulfilled resulting in a laser beam which consists out of different frequencies. For some applications demanding an extreme purity of the laser frequency to achieve a high coherence length only one mode should oscillate. This can be achieved by two means. Firstly the length of the laser cavity L is reduced and thus the distance of the modes is increased in such a way that only fits under the gain profile. However this method also reduces the length of the amplifying media resulting in low available laser power. Another method is the use of a so called etalon.

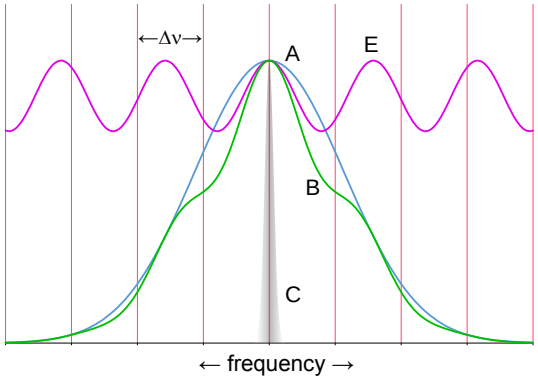

Fig. 50: The transmission profile of the etalon (E) folded with the gain curve (A) resulting in modified gain (B)

Inserted into the cavity the etalon introduces periodic extra losses with its transmission profile and modulates the net gain profile to curve (B). By selecting the right length of the etalon, which in our experiment is 1 cm, single mode operation is achieved.

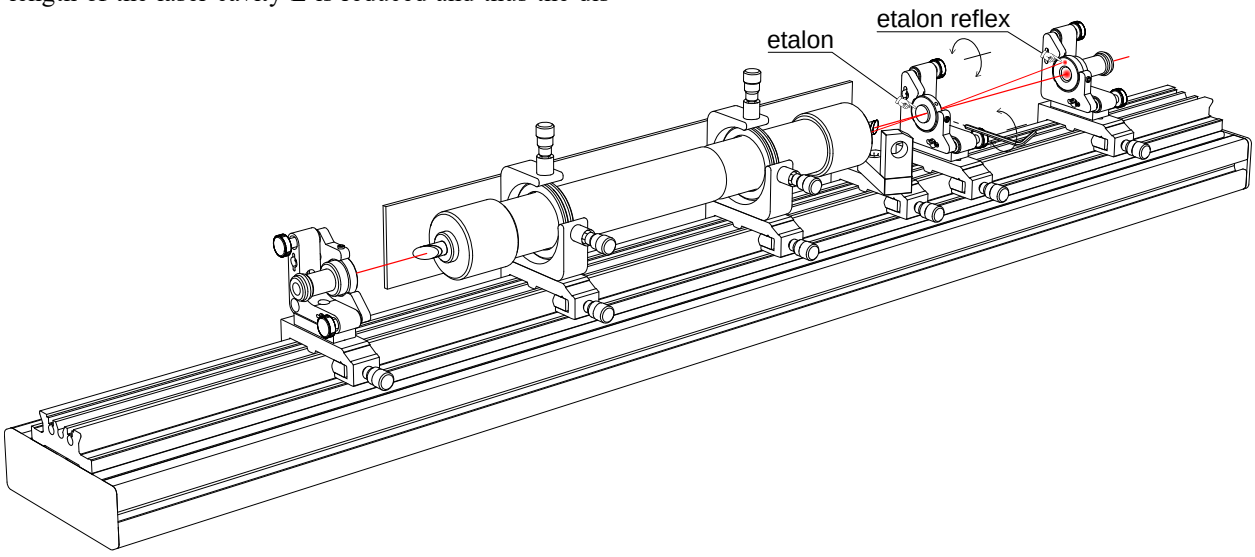

Fig. 51: The etalon is placed onto the rail

In a well optimised laser the etalon is placed as shown in [Fig. 51]. Align the etalon by turning the adjustment knobs to achieve laser oscillation. Observe the reflex which is created by the etalon in case it is not exactly vertically aligned. Align the etalon in such a way that it is aligned perpendicular. By tilting either the knob for horizontal or vertical tilt in one direction different order of the etalon are observed. That means that the laser oscillation ceases and comes back when continuing tilting.

5.10 Longitudinal modes

From the preceding chapter we already know that the experimental Helium Neon laser will operate on different longitudinal modes simultaneously. We also notice that the difference or beat frequency of two neighboured mode depends on the cavity length L (the spacing between the mirror). For a length of 1 m of the cavity we calculate a beat frequency of 150 MHz.

$$\Delta\nu = \frac{c}{2 \cdot L} = \frac{3 \cdot 10^8}{2 \cdot 1} = 150\ MHz$$

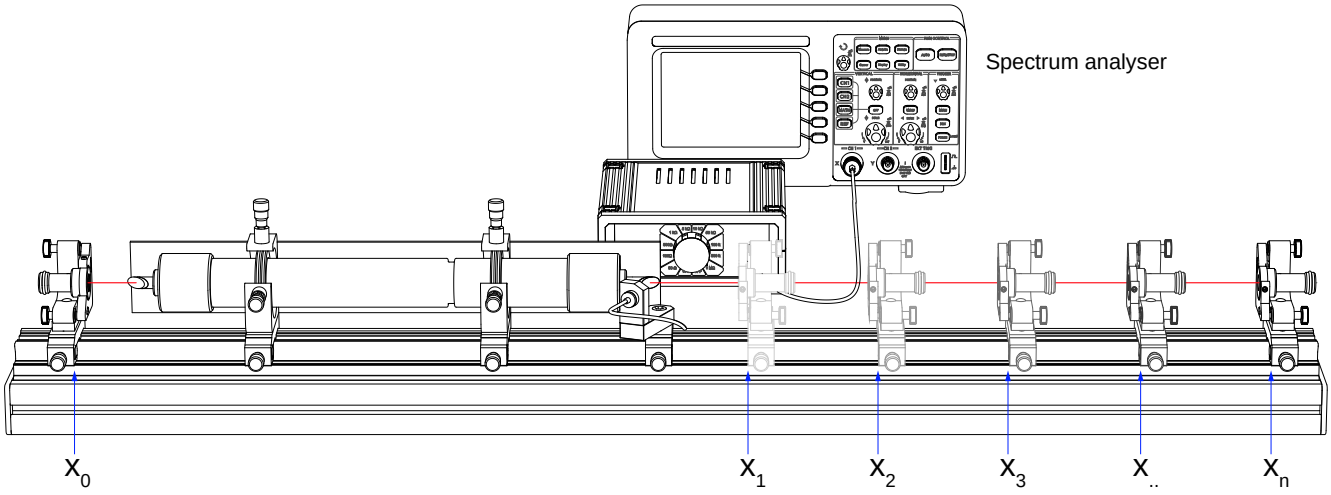

Fig. 52: Measuring the beat frequency of longitudinal modes with an electronic spectrum analyser

The provided photodetector as well as the signal conditioning box are able to detect such fast optical signals. The ZB1 box is switched to a shunt of 50 Ohms and simply connected to the spectrum analyser. Surprisingly the spectrum analyser shows beside the peak related to Δν some more peaks. Recalling that the laser oscillates on a couple of modes there will be also contributions from the over next neighbouring mode and so on. Depending on the number of oscillating longitudinal modes we will notice a progression of peaks. In the example of [Fig. 54] 5 modes are oscillating creating 4 beat frequencies. The number of beat frequencies are telling on how many modes the laser oscillates.

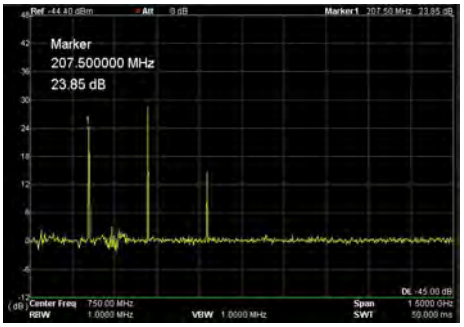

Fig. 53: Monitor display of a measurement showing beside the peak of Δν some other harmonics

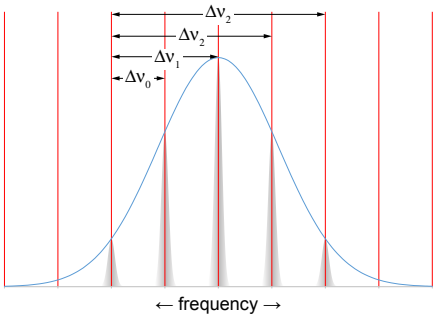

Fig. 54: Simultaneously oscillating modes creation a progression of beat frequencies

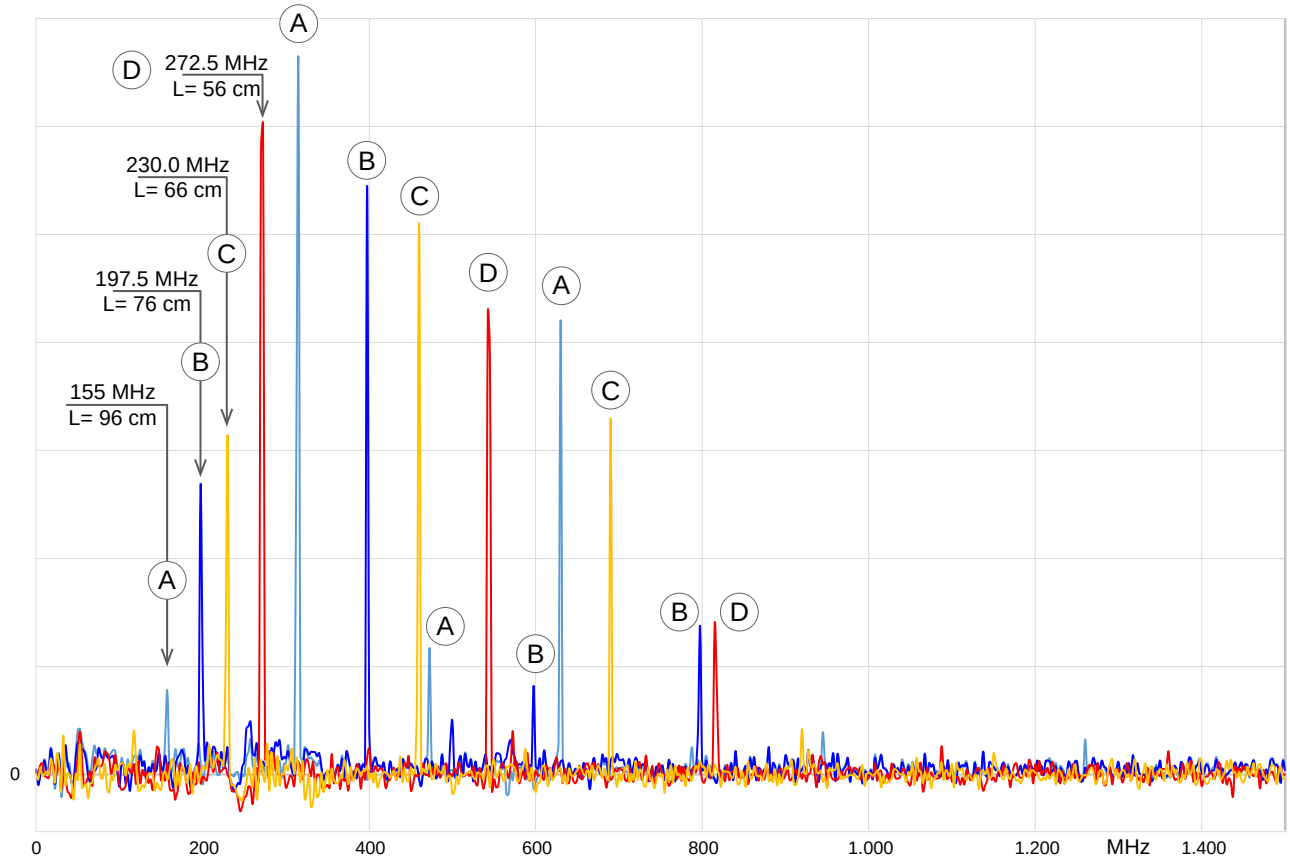

Fig. 55: Tracks of the spectrum analyser for a cavity length of 96 cm (A), 76 cm (B), 66 cm (C) and 56 cm(D)

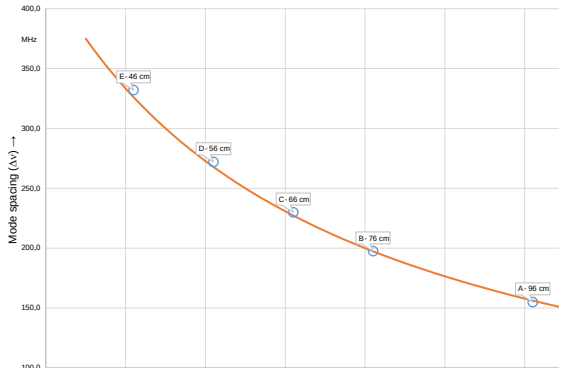

Fig. 56: Measurement of the mode beat frequency versus cavity length

By using this novel method we can study the longitudinal modes in detail by measuring its beat frequencies with a high accuracy. We can impressively verify the dependency of the beat frequency on the cavity length and can detect how many modes are oscillating. This is fascinating.

6.0 Bibliography

1. Maiman, T. H., „Stimulated Optical Radiation in Ruby“, Nature 187 4736,pp. 493-494, (1960)
2. A. L. Schawlow and C. H. Townes, „Infrared and optical masers“, Phys. Rev. 112 (6) , (1958)
3. A. Javan, “The History of the laser”, http://alijavan.mit.edu/
4. A. Javan, W. R. Bennett, D. R. Herriott: Population Inversion and Continuous Optical Maser Oscillation in a Gas Discharge Containing a He-Ne Mixture. In: Physical Review Letters. 6, Nr. 3, 1961, S. 106–110
5. Geusic, J. E.; Marcos, H. M.; Van Uitert, L. G., „Laser oscillations in Nd-doped Yttrium Aluminum, Yttrium Gallium and Gadolinium garnets“, 4 (10) 182,, 1964
6. A.D. White and J.D. Rigden, “Continuous Gas Maser Operation in the Visible”. Proc IRE vol. 50, p1697: July 1962.
7. W. Luhs, „Diode pumped Nd:YAG laser“, MEOS GmbH, 1992, http://repairfaq.ece.drexel.edu/sam/MEOS/EXP0578.pdf
8. H. KOGELNIK AND T. LI ,“Laser Beams and Resonators “ October 1966 / Vol. 5, No. 10 / APPLIED OPTICS 1
9. Safety of laser products Part 1: Equipment classification, requirements and user‘s guide, , 2001-08, http://www.ee.washington.edu/people/faculty/darling/ee436s14/IEC_60825_1.pdf
10. W. Luhs, B. Struve, and G. Litfin, “Tunable multiline He–Ne laser”, Laser Optoelectronic 18 ,319-357, 1986
11. W. Luhs, „Experiment 06 Helium Neon Laser“, MEOS GmbH, 1999, http://repairfaq.ece.drexel.edu/sam/MEOS/EXP06.pdf
12. A. E. Siegman, “LASERS”, University Science Books, 1986

7.0 Photodetector DC-0300

Introduction

Detection of light is one of the most important tasks in photonics application and research. Especially in labs and for educational tasks a kind of multimeter like the all available digital voltmeter (DVM) is required to measure optical parameter like the optical power and timely response, even of very weak and very fast signals.

In this manual we describe a new developed photodetector device which considers modern electronic equipment for signal acquisition like oscilloscopes and spectrum analyser. Meanwhile those devices reached a maturity in sensitivity (µV) and signal speed (10 GHz) for economic prices. Therefore, it makes no sense nowadays to develop a photodiode amplifier with such parameters.

Great care must be taken to shield the environmental high frequency radiation cause by radio and GSM station.

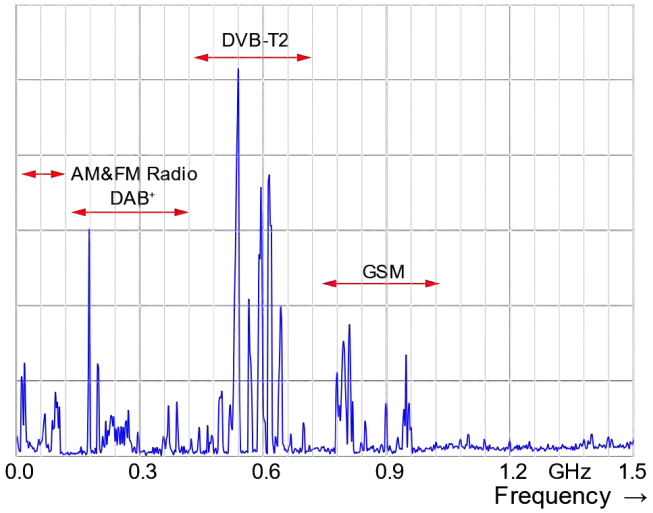

Fig. 57: Environmental Frequency Spectrum

This can only be achieved by consequential shielding of the entire detection circuitry. For this purpose, the entire inner device is encapsulated into a Faraday cage. Due to this design, it became possible to operate oscilloscopes or spectrum analysers with highest sensitivity without be bothered by unwanted high frequencies.

7.1 Theory

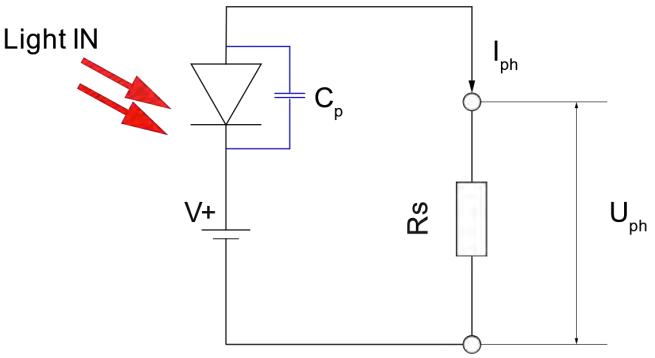

Fig. 58: Photoconductive Mode

A photodiode can be operated in two ways, either in photovoltaic or photoconductive mode. The Fig. 58 shows the photoconductive mode. If the voltage V+ is set to zero (the battery is exchanged against a short circuit), the mode is changed to the photovoltaic mode. However, the application we are targeting requires the photoconductive mode.

Photoconductive Mode

The cathode of the photodiode is supplied with a positive voltage *V+* (reverse bias). When light with power P illuminates the photodiode, a photo current I_{ph} flows through the photodiode as well as the shunt resistor Rs. The photocurrent Iph is linear to the power of the incident light and non linear to the spectral sensitivity of the photodiode (Fig. 59). The photocurrent is measured as voltage drop (Uph) across the shunt resistor.

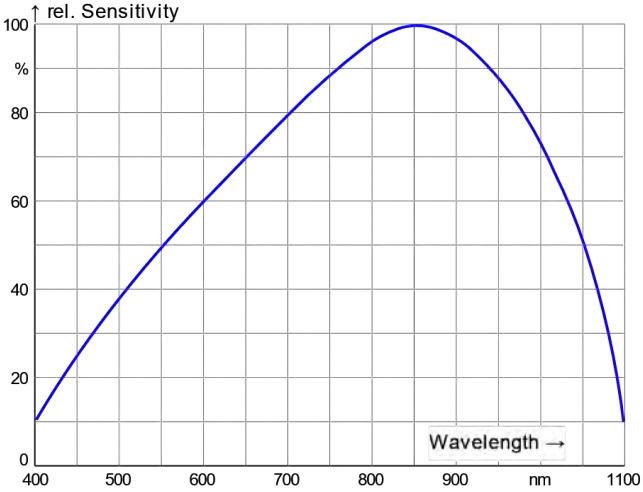

Fig. 59: Relative sensitivity S_R versus Wavelength λ, at 850 nm the absolute sensitivity S_R is 0.62 A/W

The measured photo current Iph is given by the relation:

$$I_{ph} = \frac{U_{ph}}{R_S}$$

If the wavelength is 700 nm, we obtain a value for the relative sensitivity from Relative sensitivity SR versus Wavelength λ, at 850 nm the absolute sensitivity SR is 0.62 A/W of 80% and thus an absolute sensitivity of . That means, if we measure a current of 0.5 A, the incident power is 1 W at a wavelength of 700 nm. Provided the entire light hits the sensitive detector area, the optical power Popt is given by:

$$I_{ph} = \frac{U_{ph}}{R_S}$$

It appears, that by increasing the resistance of R_S, the volt-

age U_{ph} can be arbitrary increased to achieve a high sensitivity. This in principle true, however, at the cost of frequency bandwidth. The pn transition of the photodiode has an unavoidable parasitic capacity Cp which depends on the applied reverse bias (Fig. 59).

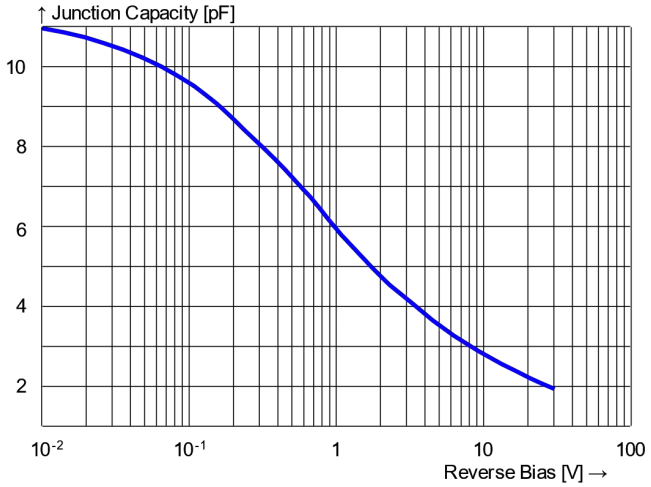

Fig. 60: Junction Capacity versus Reverse Bias V+

$$f_{BW} = \frac{1}{2 \cdot \pi \cdot R_S \cdot C_p}$$

For Cp= 2.9 pF at 9V (see Fig. 59) and RS=50 Ohms the bandwidth fBW amounts to 1.14 GHz.

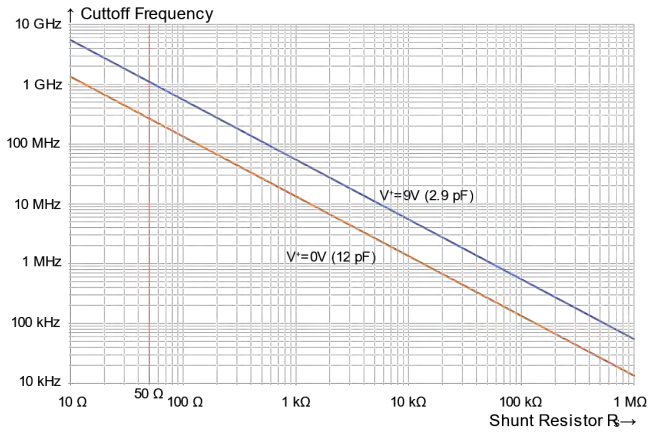

Fig. 61: Cutoff frequency f_{BW} versus shunt resistor RS

For low values of the shunt resistor R_S the detector is very fast but has a low sensitivity. For higher values for the shunt resistor the speed is reduced, but the sensitivity increases.

7.2 Device Properties

The aim of the DC-0300 is to provide an instrument which allows to detect extremely fast signal up to 1.5 GHz and very low intensities down to a few nW. This requires selectable shunt resistors in a range from 10 Ω to 1 MΩ.

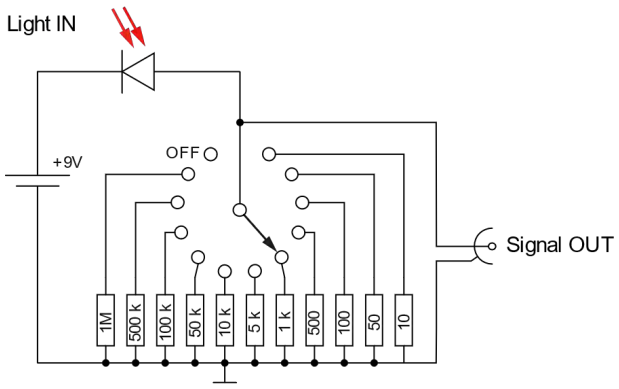

Fig. 62: Basic electronic design of the DC-0300

Each element of the circuitry may act as an antenna for external electromagnetic interference (EMI) superimposing the measurement signal.
To achieve the best shielding against EMI created by local radio stations, cellular phones, wireless LAN as well as terrestrial digital broadcast services, the entire circuit must be placed into a Faraday cage.

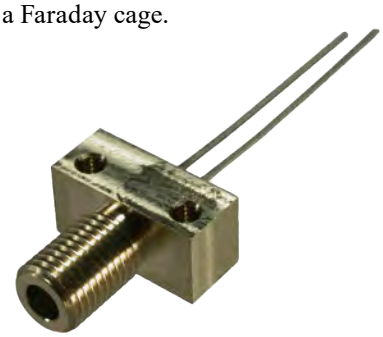

Fig. 63: Shielded SiPIN photodiode

It starts with an encapsulated photodiode which is placed into a Faraday cage behind the front plate. The thread (F-SMA) is used to mount the photodiode to the front plate and to accommodate an optical fibre. The used photodiode is a Si PIN diode with an active area of 1 mm² and is encapsulated into a metal housing.

Fig. 64: DC-0300 Front view

The signal output is available at a BNC jack (Signal OUT) at the front plate. The rotary switch selects the desired shunt resistor RS.

Fig. 65: DC-0300 Rear view

At the rear panel, the 9V battery providing the reverse bias is accessible for replacement. The battery has a capacity TR of 550 mAh. Assuming a photocurrent Iph of 1 mA (which is remarkably high), the lifetime for continuous operation is 550 hours.

$$T = \frac{T_R}{I_{ph}} = \frac{550\,mA}{1\,mA} = 550h$$

In principle an external power supply could be used to provide the reverse bias. However, almost all power supplies are creating parasitic radiation, which limits the lowest sensitivity of the photodetector. That is why we prefer using a battery.

7.3 Example Measurements

7.3.1 DC Measurements

Fig. 66: Fig. 3.5: Measurement with a digital voltmeter

For pure DC measurements the DC-0300 is connected to a DVM by means of the provided BNC to Banana plug adapter.

7.3.2 Oscilloscope Measurements

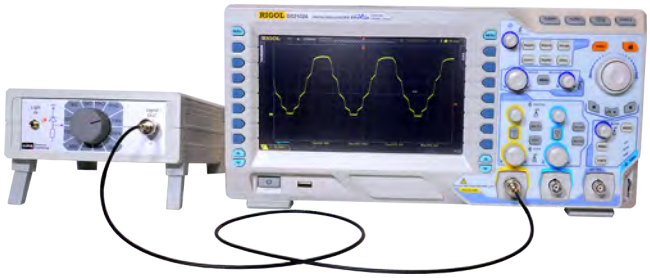

Fig. 67: Measurement environmental light (LED beamer) with an oscilloscope

Without optical fiber the environmental light which enters the panel F-SMA jack is measured (Fig. 67 Measurement environmental light (LED beamer) with an oscilloscope).
By using the fiber patch cable, the emission of other light sources can be measured. The Scope trace of a 12 ns diode laser pulse shows such an example. The light of a pulsed diode laser was directed to the F-SMA fiber jack located at the front panel of the DC-0300.

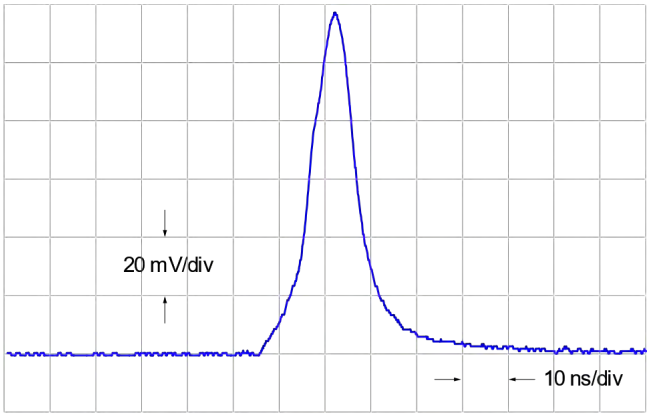

Fig. 68: Scope trace of a 12 ns diode laser pulse

The electronic pulse width was set to 12 ns. The Scope trace of a 12 ns diode laser pulse shows the optical response measured with the DC-0300.

7.3.3 Spectral Measurements

Due to the high spectral bandwidth (0-1.5 GHz), corresponding fast optical radiation can be detected.

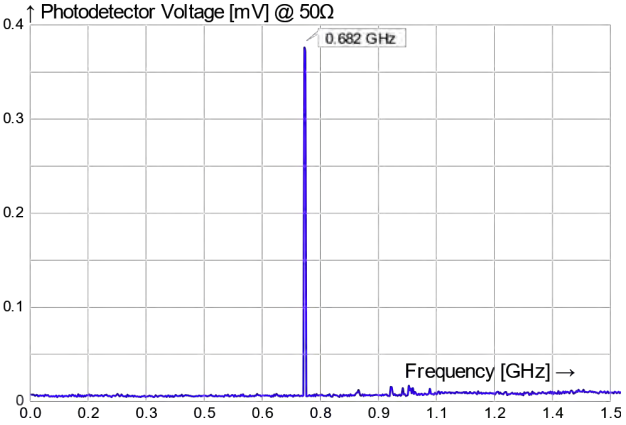

Fig. 69: Beat frequency signal of a two mode HeNe laser

The example of Beat frequency signal of a two mode HeNe laser shows the trace of an electronic spectrum analyser. The light of a two mode HeNe laser is captured by the optical fibre and the output of the DC-0300 is connected to the spectrum analyser.